THERMODYNAMICS AND STATISTICS OF THE ELECTRON GAS

3. THERMODYNAMICS OF THE ELECTRON FLOW
4. DETERMINATION OF THE ELECTRON TEMPERATURE

N6–ori–71 Task XIX
NR 073 162
TECHNICAL REPORT No. 3-3; 3-4

ELECTRICAL ENGINEERING RESEARCH LABORATORY
ENGINEERING EXPERIMENT STATION
UNIVERSITY OF ILLINOIS
URBANA, ILLINOIS

THERMODYNAMICS AND STATISTICS OF THE ELECTRON GAS

3-3. THERMODYNAMICS OF THE ELECTRON FLOW

3-4. DETERMINATION OF THE ELECTRON TEMPERATURE

N6-ori-71 Task XIX
Technical Report No. 3-3; 3-4.
NR-073-162

Date:
June 1954

Sponsored by:

United States Navy
Office of Naval Research

Prepared by:

T.N. Chin

Approved by:

H.M. Von Foerster
Professor

ELECTRON TUBE SECTION
ELECTRICAL ENGINEERING RESEARCH LABORATORY
ENGINEERING EXPERIMENT STATION
UNIVERSITY OF ILLINOIS
URBANA, ILLINOIS

TABLE OF CONTENTS

	Page
Part I - Thermodynamics of the Electron Flow	1
1. Introduction	2
2. The Problem and the Method of Solution	8
3. Two Essential Types of Flow	18
3.1 Anisotropic Flow	23
3.2 Isotropic Flow	26
Appendix I. Derivation of the Flow Equations.	32
Appendix II. Functional Relationship Between the Electron Temperature and the Mean Velocity.	36
Appendix III. Evaluation of the Constants at the Emission Surface.	40
Appendix IV. Solution of the Equation.	44
Part II - Determination of Electron Temperature	47
1. Introduction	48
2. Theoretical Considerations	49
3. Experimental Apparatus	55
4. Estimation of Aberrations	59
4.1 Electron Lens Effect	59
4.2 Space Charge Effect	61
4.3 Secondary Electron Effect	63
4.4 Conclusion	68
4.5 Experimental Results	68
Bibliography	80
Distribution List	

ILLUSTRATIONS

Figure Number		*Page*
	Part I	
1	Characteristic Form of the Potential Distribution in a Parallel Plane Diode	4
2	Associated Transmission Coefficient	4
3	The Plot of T_{fl} and λ Close to the Emission Surface Against the Cathode Temperature	27
4	Electron Temperature Components vs. Mean Velocity	37
5	Electron Temperature Components vs. Distance from the Cathode Surface	39
	PART II	
1	Schematic Diagram of the Experimental Setup to Measure the Radial Component of the Electron Temperature	50
2	Beam Expansion Due to Electron Temperature	51
3	R-Component Temperature Analyzer	56-57
4	Application of Gauss' Theorem to a Circular Aperture	58
5	Divergent Action of a Single Aperture	62
6	Polar Angles as a Function of the Ratio D/R_o	62
7	Diagram of the Anode Orifice	63
8	Secondary Electron Emission from an Orifice	64
9	Value of $\sin^2\theta \cos^3\theta$ as a Function of θ	67
10	Reduced Current Density as a Function of Cathode-Anode Spacing	69
11	Reduced Current Density as a Function of Anode Potential	70
12	$\frac{J(\theta)}{J(0)}$ vs. θ^2	73
13	$k\Theta_r$ vs. the Distance from the Cathode Surface	75
14	$k\Theta_r$ vs. Current Density	77
15	Relation Between Electron Temperature and Cathode Temperature	77
16	Illustrative Diagram of the Oxide Coating	79

LIST OF SYMBOLS

1. Geometrical Quantities

$\vec{r}$ - the space vector in the rectangular coordinates

x_1, x_2 and x_3 - the components of the space vector in the rectangular coordinates

x - the coordinate along the electron flow

t - the time variable

z - cylindrical coordinate along with the electron flow

r - the radial distance from the z-axis

R - the radial distance in the spherical coordinates which takes the center of the anode orifice as the origin

θ - the polar angle of the spherical coordinates

Φ - the azimuthal angle of the spherical coordinates

δ - an incremental polar angle from θ

Ω - the solid angle in the unprimed coordinates

Ω' - the solid angle in the primed coordinates

l_1 - the length of the cylinder to the left of the anode plane

l_2 - the length of the cylinder to the right of the anode plane

D - the cathode-anode spacing of the diode

θ_1 - the polar angle that the expanded beam at the back wall (due to electron lens effect alone) would subtend at the origin

θ_2 - the polar angle that the expanded beam at the back wall (due to space charge effect alone) would subtend at the origin

γ - r/r_0, the ratio of the radius of the electron beam at the z-plane and that of the anode orifice.

2. Electrical Quantities

V - the potential in volts

ρ - the charge density in the electron flow

J - the electric current density

$\vec{F}$ - the force per unit mass of electrons

n - the number density of the electrons at a point in the flow

E - the applied electric field

E_1 - the electric field at the left end of the cylinder

E_2 - the electric field at the right end of the cylinder

E_r - the radial components of the electrical field across the mantel surface

j_A - the anode current density in $\mu a/cm^2$

I_o - the total current through the anode orifice

I_p - the primary electron current to the inner wall of the anode orifice

I_s - the secondary electron current from the inner wall of the anode orifice

i_s - the secondary electron current per unit area of plane surface

$j(\theta,\delta)$ - the current between the concentric cones with the apex angles 2θ and $2(\theta + \delta)$ per unit area of the anode orifice

$J(\theta,\delta)$ - the current density at the Z-plane between the polar angles θ and $(\theta + \delta)$

$J(\theta)$ - the current density at the Z-plane with a polar angle θ

$J_s(\theta)$ - the current density at the Z-plane with a polar angle θ due to secondary electrons alone

W - the work function of the emission surface

T - the cathode temperature

R_s - the ratio of the space charge current to the current emission of the cathode

3 Dynamic Variables

v_o - the initial velocity of the electrons at the cathode

v_x - the velocity of the electrons at point x

$\vec{c}$ - the velocity vector of an electron in the rectangular coordinates

c_1, c_2 and c_3 the velocity components with respect to the rectangular coordinates

c_r - the r-component velocity of the electron

c_z - the z-component velocity of the electron

$\vec{u}$ - the vector of the peculiar velocity of an electron

$\vec{c}$ - the mean velocity of the electrons at a point

v - the mean velocity along the electron flow

ψ_s - the summational invariants

τ_T - the mean transit time

τ_R - the relaxation time

λ - the mean free path

Θ - the electron temperature generally a tensor at a point in the electron flow

Θ_1, Θ_2, Θ_3 - the diagonal components of the electron temperature tensor

Θ_z - the z-component of the electron temperature

Θ_r - the r-component of the electron temperature

f, φ - the velocity distribution functions of the electrons at a point in the electron flow

4. Constants

m - the mass of an electron ($9.10\ (10)^{-28}$ gm.)

e - the charge of an electron ($4.80\ (10)^{-10}$ e.s.u.)

k - a Boltzmann constant ($1.38\ (10)^{-16}$ erg/degree)

r_o - the radius of the anode orifice (0.00675 inch)

Z - the coordinate of the back wall of the anode chamber, ($Z = 1.200$ inch)

t_W - the thickness of the anode wall ($r_o/3$)

Q - the proportional constant in the Child-Langmuir space-charge law

η - $\frac{mu^2}{2k\Theta_r}$, the ratio of the mean energy and the internal energy of the electrons at a point in the electron flow

ε - the normal-energy constant of an emission surface

A, B, G, L and M - constants in the equations

h, h' and H - the proportionality constants in the equations of secondary electron emission.

PART I

THERMODYNAMICS OF THE ELECTRON FLOW

1. INTRODUCTION

In the following pages, the electron flow in a diodic arrangement will be treated from a general point of view. To elucidate an essential feature of the physical behavior of the diode, a different viewpoint will be taken at the very beginning. In contrast to the usual representation where, at a constant cathode temperature, the anode potential is varied and the anode current is taken, we shall consider here the case where the anode potential is kept constant but the cathode temperature is raised. Thus, if a constant positive anode potential is applied and the cathode temperature is gradually raised, the current in the diode will first ascend quickly and then reach saturation with further increase of the cathode temperature. This fact leads to the conclusion that many of the emitted electrons are forced to return to the cathode when the current reaches the saturation. The interpretation of this behavior is that in spite of the existence of a positive potential on the anode, the high accumulation of space charge in front of the cathode may still depress the potential there so low that a considerable amount of emitted electrons will return to the cathode.

In the process of developing an adequate quantitative description of the physical behavior of the diode, two phases can be distinguished in the papers of the early workers in this field which successfully explain several features of the diode. The problem was first studied[1] under the assumption that all the electrons leave the cathode with the same initial velocity and are accelerated in exactly the same manner in the diode. In other words, the electron velocity at any point in the diode is considered as being single-valued. Then the problem may be attacked only from Poisson's equation, the energy equation and the relation between current, charge and velocity, namely,

$$\frac{d^2V}{dx^2} = -4\pi\rho \tag{1}$$

$$\frac{1}{2}mv_x^2 - \frac{1}{2}mv_o^2 = eV \tag{2}$$

$$J = \rho v_x \tag{3}$$

where x is the distance from the cathode measured perpendicular to the plane of the cathode, v_x is the velocity of the electron at a point x, v_o is the initial velocity of the electron at the cathode, V is the

potential at any point determined with respect to the cathode, e and m are the charge and mass of the electron, ρ and J are the charge and current densities. The solution thus obtained is certainly not general and, at best, may be applicable only to the case where all the electrons at any one point are moving in the same direction.

The essential work in the second phase was done by Epstein[2], Fry[3] and Langmuir[4]. Instead of assuming the electron velocity to be single-valued in the diode, they considered a velocity distribution of the emitted electrons at the cathode surface. The usual representation of the potential distribution in a diode is given in Fig. 1. The potential depression in front of the cathode is particularly emphasized in this figure. If the potential minimum is found, one can determine precisely the trajectories of all electrons after they are emitted from the cathode. The interpretation was that those electrons with initial kinetic energy higher than the potential minimum would come through to the anode and those with less initial kinetic energy would return to the cathode. It can be said to the merit of Epstein, that he brought up two questions: a: What distribution function one must use to describe the current emission in terms of the initial velocity of the emitted electrons; b: Where one must consider the problem of encounters between electrons and electrons. Unfortunately, he did not attempt to solve the electron flow problem taking encounters into consideration, but rather assumed that the electrons are unaffected by each other throughout the electron flow in the diode. On the other hand, he was forced to treat the electron gas between the two electrodes as being in an equilibrium state which would, of course, demand that an energy exchange take place between the particles of which this gas is composed.

To form a description of the gas under consideration which would come as close as possible to the actual behavior of the electrons in the diodic arrangement, one should consider all the effects expected to contribute essentially to the overall behavior of the electron gas under the conditions in question. Three microscopic phenomena will be considered as the decisive factors in the determination of the macroscopic behavior of the electron gas.

First, one has to consider the change of particle density with respect to the space coordinates due to the accelerated motion of the particles between the cathode and the anode. Examination of the parti-

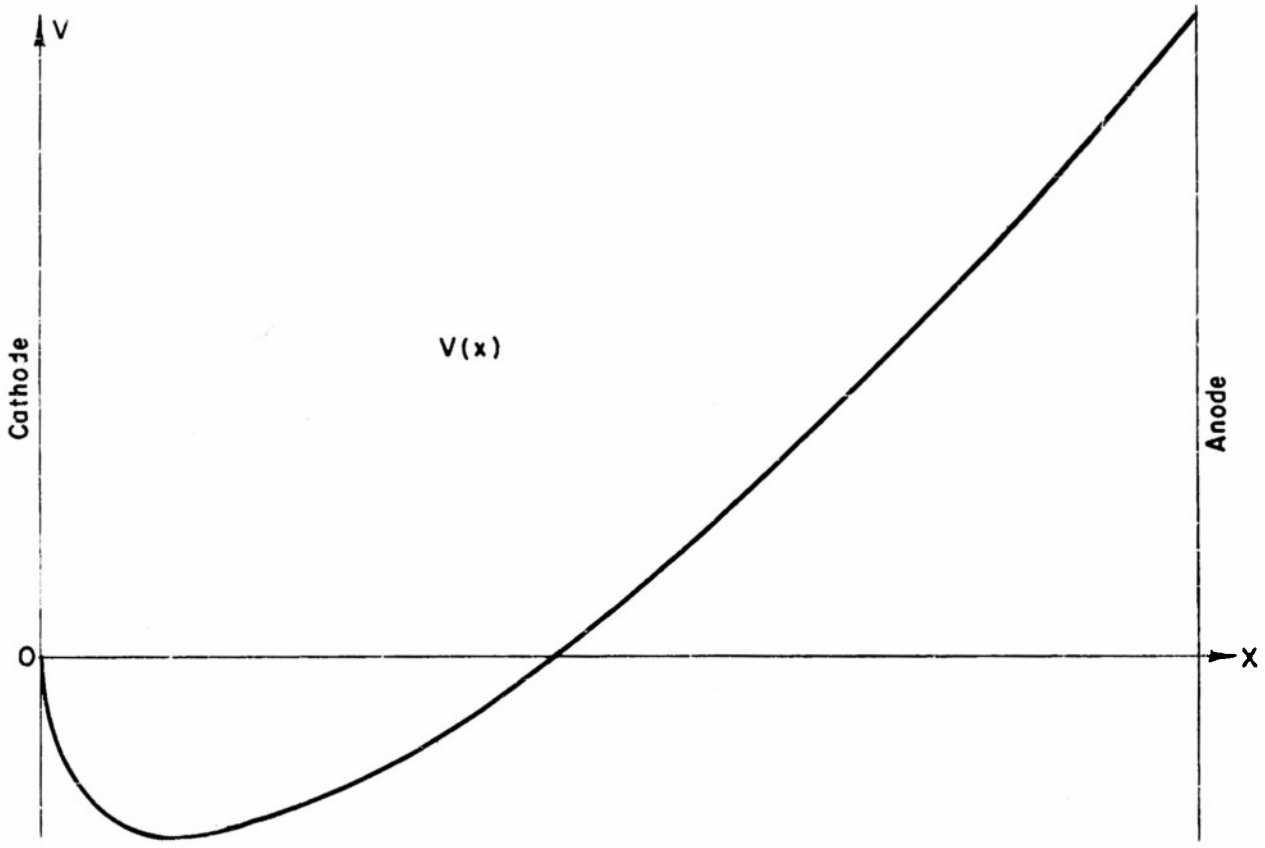

FIGURE 1 CHARACTERISTIC FORM OF THE POTENTIAL DISTRIBUTION IN A PARALLEL PLANE DIODE

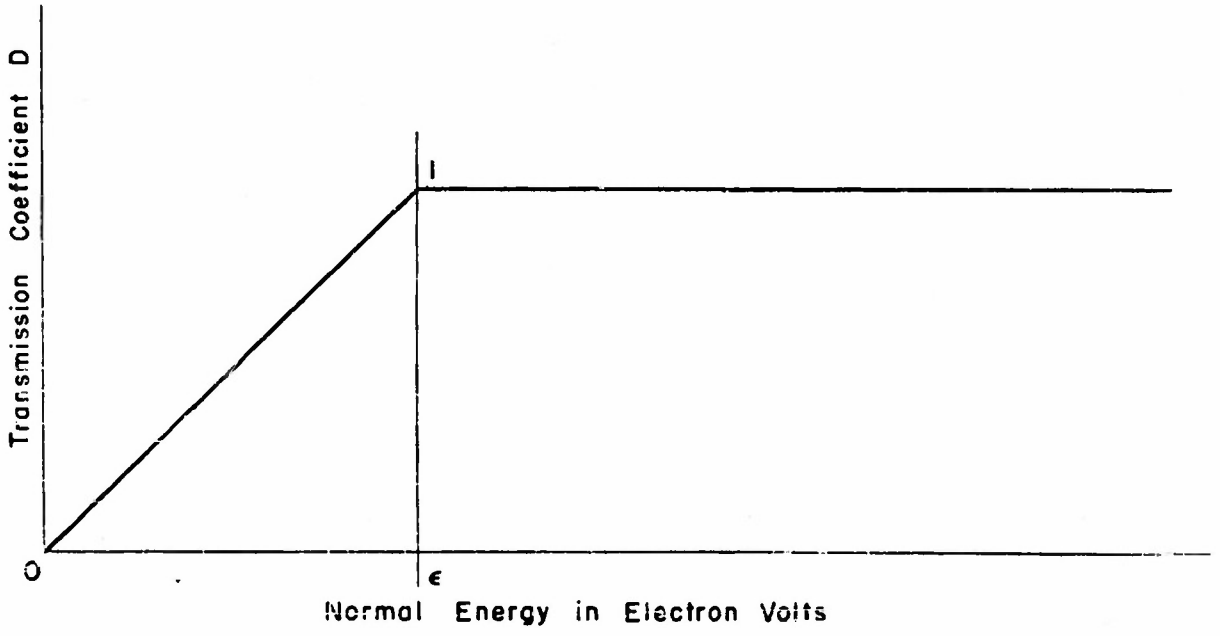

FIGURE 2 ASSOCIATED TRANSMISSION COEFFICIENT

cles at any fixed location in the flow, shows eac' of them moving in a different direction with a different velocity. The usual method is to decompose the velocity of each particle into two vectors, one being the mean velocity which is the same for all the particles at that location, and the other being the spread velocity of that particular particle with respect to the mean velocity. Thus the particles at that location in the flow will have a mean velocity on which the velocity spread is superimposed.

Next, one has to consider the external forces acting on the particles and the change of particle density with respect to their three velocity components. These three velocity components together with their corresponding space coordinates constitute in the usual way the phase space (μ-space) for that gas. The external forces acting on the particles are those due to sources outside the location of the particles in consideration.

Finally, in case of an electron gas, the internal forces acting on the particles in question must be also considered. These interanl forces are produced by the interactions between the particles which are very close together. From a statistical point of view, it is believed that the effect of these interactions can best be described by a concept of encounters between the different particles. Since the treatment of that problem in this paper includes the effect of the internal forces on the process of encounters, the precise meaning of the potential[5] will be one from which only the external forces are derivable.

The best tool to describe such a gas at any point within the flow is the Boltzmann equation:

$$\frac{\partial f}{\partial t} = - \vec{c} \cdot \nabla_{\vec{r}} f - \vec{F} \cdot \nabla_{\vec{c}} f + \frac{\partial_e f}{\partial t} \qquad (4)$$

where the velocity distribution function f is the dependent variable, but $\vec{F}$, $\vec{c}$, $\vec{r}$ and t are independent variables. It is clear that $\frac{\partial f}{\partial t}$ is the rate of change in time of the velocity distribution function, whereas $\vec{F}$ is the external force per unit mass, ∇_r and ∇_c denote the del operators with respect to space coordinates and velocity coordinates respectively. The quantity $\frac{\partial_e f}{\partial t}$ written in Eq. (4) is the rate of change of the velocity distribution function due to the encounters of the particles, and thereby is the result of all particle encounters at the location in

consideration. Hence the expression $\frac{\partial_e f}{\partial t}$ is an integral involving the unknown function f ($\vec{c}$, $\vec{r}$, t) of the problem. So Boltzmann's equation is an integro-differential equation which indicates that the change of the velocity distribution function at any point within the flow comes from three sources that are precisely the three factors listed above. Since the first term of the right hand side of Eq. (4) points out the non-uniformity of the flow of the gas under consideration, the methods adopted in this treatise will be similar to those developed by workers dealing with non-uniform gases. Particularly, the nomenclature will follow the one given by Chapman and Cowling[6].

It will be shown that the electron flow between the cathode and the anode can be completely described with four macroscopic quantities. These four quantities are:

1. External force field $\vec{F}$
2. Electron number density n
3. Mean velocity $\vec{c}$
4. Electron temperature Θ

The temperature of a gas in general may be expressed as a second-order tensor, which is an array of nine ordered components. In this paper, however, the electron temperature consists of only three mutually perpendicular components, Θ_1, Θ_2 and Θ_3, which are calculated from the velocity distribution of electrons in the rectilinear flow. In a molecular gas where these three components are always equal, the temperature may be further degenerated into one component, thus a scalar.

In a later part of this report, two examples will be given of how the presented theory can be applied to certain flow problems. In particular two cases will be distinguished: the one in which the three temperature components, Θ_1, Θ_2 and Θ_3, are equal to each other but vary only with the location in the flow, which will be properly called the "isotropic flow"; the other one, in which the temperature component in the direction of flow, Θ_1, will vary with the location in the flow; but the other two components perpendicular to the flow, Θ_2 and Θ_3, will be constant throughout the flow, hence different from Θ_1. Accordingly this case will be termed the "anisotropic flow".

In this treatise, the effect of magnetic fields will be neglected. This approach will finally yield exact solutions for the steady state.

The solutions will degenerate to known expressions obtained from the single-valued velocity theory if the effect of encounters is neglected. All equations, except when explicitly noted otherwise, are written in electrostatic units, centimeters, grams, and seconds.

II. THE PROBLEM AND THE METHOD OF SOLUTION

In the preceding section, it was pointed out that an adequate tool to describe the behavior of the electron gas in the condition of diodic flow would be Boltzmann's integro-differential Eq. (4). This would account for mutual interaction of the particles by the way of encounters. From a practical point of view, the condition of the flow after it has attained its steady state should deserve first attention rather than the very general case of studying the transients of this flow. This enables one to make a considerable simplification of the very complex task of solving generally Eq. (4), since it becomes unnecessary to account for a change in time of the VDF* at a particular point in consideration. That precisely means that

$$\frac{\partial f}{\partial t} = 0 \tag{5}$$

if only the steady state is considered. Since from now on only the steady-state case is considered, the problem should be to solve the steady-state Boltzmann equation

$$\vec{c} \cdot \nabla_r f + \vec{F} \cdot \nabla_c f - \frac{\partial_e f}{\partial t} = 0 \tag{6}$$

for the VDF at any point within the flow. That precisely means, to find uniquely an

$$f(\vec{c},\ \vec{r},\ f_o(\vec{r}_o))$$

which would satisfy Eq. (6), where, because of the character of this particular equation -- being linear and of the first order -- one has a free choice of the distribution function at a particular point in the flow. This boundary condition was formerly introduced as $f_o(\vec{r}_o)$.

It is well known to workers in this field that an attempt to solve generally the Boltzmann equation leads to insurmountable mathematical difficulties, even in the simplified form of Eq. (6), where only the steady-state case is considered. In spite of this fact, several methods were devised to solve this equation for some particular cases.

One of the early simplifying restrictions imposed upon the problem was the condition of uniformity and steadiness of the gas under consideration. This means, a.) no external force, b.) zero mean velocity.

*VDF, hereafter stands for velocity distribution function.

The solution for f in this case is, of course, the well known Maxwellian VDF.

Recently, Kihara[7] studied the case where the gas under consideration was composed of charged and uncharged particles. In the case where the number of uncharged particles is much larger than the number of charged particles, the collisions among charged particles can be considered negligible in comparison with the collisions of charged with uncharged particles. Solutions are obtained with a further restriction, namely, that the drift velocity of the charged particles is small in comparison with their thermal velocity. Obviously, the restriction pointed out above cannot be imposed upon the case considered in this paper, that of the flow of an electron gas in a high vacuum diode. Unfortunately, there is at present no precise mathematical expression to describe adequately the phenomenon of encounters between electrons. Even with an approximate expression for the term, $\frac{\partial_e f}{\partial t}$, symbolizing the encounters in the Boltzmann Eq. (6), one still meets insurmountable mathematical difficulties to find a solution for f.

No attempt will be made in this paper to solve for the VDF under particular restrictions imposed upon the problem. The method suggested here will be to define a class of VDF's by stating properly the physical properties of the flow and then selecting a representative function of this class of VDF's which may contain the "true function" as one of its members. It will be seen that the so selected VDF will approach any function of that class within the third moment.

In the course of describing the physical properties of the flow and defining in that way the class of VDF's, any member of which will serve as an approximation to the "true function" up to the third moment, one links the microscopical quantities defining the VDF with macroscopic quantities accessible to measurements, as was mentioned in the preceding section.

Let $\vec{c}$ be the linear velocity in coordinates fixed with respect to an observer in the laboratory. Then the electron number density in the neighborhood of a point $\vec{r}$ in the flow is given by

$$n(\vec{r}) = \int f(\vec{c},\vec{r})\, d\vec{c} \tag{7}$$

where, here and in the future, a notation $\int \cdots d\vec{a}$ indicates an integra-

tion carried out over all components of the vector quantity $\vec{a}$ in the entire $\vec{a}$ space.

In accordance with the usual definition of the mean value of an arbitrary function with respect to a distribution function f, the mean value $\bar{\vec{c}}$ of the function $\vec{c}$, the velocity of the electrons in the flow, will be defined as

$$\bar{\vec{c}} = \frac{1}{n} \int \vec{c}\ f\ (\vec{c},\vec{r})\ d\vec{c} \tag{8}$$

Eqs. (7) and (8) will impose some restrictions as to the free choice of an arbitrary VDF, since any suggested VDF must be consistent with the conditions defined in Eqs. (7) and (8). Since these equations are the definitions of the zero and the first moments of the velocity distribution function f, at that state of the development, it can be said that such a function f satisfying (6), (7) and (8) would approximate the "true function" up to the first moment.

In a later development it will be necessary to look at the velocity distribution of the electrons in the flow from the viewpoint of an observer moving with the mean velocity $\bar{\vec{c}}$ along with the electron flow. Let $\vec{u}$ be the linear velocity in coordinates fixed with respect to this observer. Then the electron number density in the neighborhood of a point $\vec{r}$ in the flow is given according to (7)

$$n\ (\vec{r}) = \int \varphi\ (\vec{u},\vec{r})\ d\vec{u} \tag{9}$$

where $\varphi(\vec{u},\vec{r})$ denotes the VDF as observed by the moving observer, and $\vec{u}$, the peculiar velocity of the electrons in this frame of reference, is defined by

$$\vec{u} = \vec{c} - \bar{\vec{c}} \tag{10}$$

Having made clear the definition of the zero and first moments, we now proceed to consider the second moment of the VDF. By the second moment of the VDF is meant the following quantity:

$$\int \vec{u}\,\vec{u}\ \varphi\ (\vec{u},\vec{r})\ d\vec{u}$$

where the symbol $\vec{u}\vec{u}$ has been used to stress the fact that any two components of the peculiar velocity u can be combined to form a second

order term with respect to their velocity. Hence $\vec{u}\vec{u}$ can be considered as a tensor with the nine ordered components:

$$\begin{pmatrix} u_1 u_1 & u_1 u_2 & u_1 u_3 \\ u_2 u_1 & u_2 u_2 & u_2 u_3 \\ u_3 u_1 & u_3 u_2 & u_3 u_3 \end{pmatrix}$$

This makes it obvious that the second moment has the properties of a tensor, the components of which, multiplied by a constant factor $\frac{m}{kn}$, conveniently define a new tensor

$$\Theta(\vec{r}) = \frac{m}{kn} \int \vec{u}\,\vec{u}\,\varphi(\vec{u},\vec{r})\,d\vec{u} \qquad (11)$$

which is generally known as the temperature tensor in the neighborhood of the point $\vec{r}$ in the flow.

Since our aim is to obtain results from the presented theory which are applicable to practical situations, structures with rectilinear electron flow (as concentric, coaxial, parallel plane structures) will certainly receive first attention. Restricting oneself to the general class of structures with rectilinear flow, a convenient choice of the coordinates can be made by placing one axis parallel and the other two axes perpendicular to the flow. The axis parallel to the flow in the following will be labeled with index 1, the other two, 2 and 3. The necessary and sufficient condition to characterize rectilinear flow is to say that the net transport of matter is carried out along one and only one fixed coordinate. Explicitly, this means that the mean velocity, $\vec{c}$, of the flow is parallel to the external force field $\vec{F}$ in the flow. This immediately implies a simplification of Eq. (8), which defines the mean velocity in all different directions of the flow. With the particular choice of the coordinate system as described above, it follows that

$$\int u_1 \varphi(\vec{u},\vec{r})\,du_1 = 0\,, \qquad i = 2,3 \qquad (12)$$

The choice of this particular geometry, with its symmetry properties expressed through Eq. (12), has a most important bearing on the structure of the temperature tensor Θ defined by Eq. (11). A glimpse of the tensor array for the $u_i u_j$ terms indicates immediately that all the

non-diagonal terms will vanish and the temperature tensor Θ reduces to

$$\Theta = \begin{pmatrix} \Theta_1 & 0 & 0 \\ 0 & \Theta_2 & 0 \\ 0 & 0 & \Theta_3 \end{pmatrix} \tag{13}$$

Since each of the diagonal terms represents the mean square of a velocity component, the electron temperature is merely a measure of the mean kinetic energy with respect to an observer moving with the mean velocity $\bar{\vec{c}}$ along with the flow. This definition of temperature will be, of course, in agreement with that in thermodynamics when the particles under consideration reach the state of equilibrium.

Having now properly interpreted the physical significance of the second moment, we are ready to turn our attention to the third moment of the VDF. In accordance with the usual definition, one can write for M_3, the third moment:

$$M_3 = \int \vec{u}^3 \varphi (\vec{u}, \vec{r}) \, d\vec{u}$$

M_3 can be interpreted as the rate of net flow of the kinetic energy with respect to an observer moving with the mean velocity $\bar{\vec{c}}$ along with the electron flow. It will be seen later in the development, but also may be worth noting here that in practical situations the average velocity with respect to such a moving observer is much smaller than the mean velocity $\bar{\vec{c}}$ of the electron flow. The net flow of the kinetic energy with respect to such a moving observer is consequently much smaller than the flow of the kinetic energy with the mean velocity $\bar{\vec{c}}$. That is

$$\frac{k\Theta}{2} << \frac{m \bar{\vec{c}}^2}{2}$$

For this reason, the third moment M_3 can be considered to be zero, thus:

$$\int \vec{u}^3 \varphi (\vec{u}, \vec{r}) \, d\vec{u} = 0 \tag{14}$$

It may be noted that every even VDF would automatically satisfy the condition expressed in Eq. (14). However, Eq. (14) does not necessarily restrict VDF's to be even functions of $\vec{u}$. This minor restriction imposed upon the problem does not prevent us from including a vast number of functions in the class of possible VDF's and just enables us to procure solutions for the present problem.

Since all the statements so far regarding the physical properties of the electron flow have been so general that they can be considered valid whether encounters or no encounters between the particles take place, we must now turn our attention to the more specific knowledge one can obtain if one considers that even if encounters have a major role in the physics of the flow, one is able to select certain quantities which will not change before and after the encounters. Although no detailed picture of the process of encounters may ever be obtained, it is at once evident that, for example, the number of particles engaged in mutual encounters will remain constant before and after their interactions. Similarly, it is clear that the total momentum and energy of the participating particles will remain invariant during this process. Those quantities remaining unchanged during the complex process of encounters are generally known as summational invariants. Their invariability gives some additional bits of information to a sufficient description of the physical properties of the flow.

To state the three previously indicated conditions in mathematical terms one has to remember that the symbol $\frac{\partial_e f}{\partial t}$ in the Boltzmann Eq. (6) denotes the change of the VDF due to the particle encounters. Thus, the statement that the number of particles engaged in mutual encounters will remain constant before and after their interactions, can be written as

$$\int \frac{\partial_e f}{\partial t} \, d\vec{c} = 0 \tag{15}$$

Similarly, the statement that the total momentum and energy of the participating particles will remain unchanged through the encounter process, can be written

$$\int m\vec{c} \, \frac{\partial_e f}{\partial t} \, d\vec{c} = 0 \tag{16}$$

$$\int \frac{m\vec{c}^2}{2} \, \frac{\partial_e f}{\partial t} \, d\vec{c} = 0 \tag{17}$$

In general, for any function ψ which should remain unchanged during encounters, one can write

$$\int \psi \, \frac{\partial_e f}{\partial t} \, d\vec{c} = 0 \tag{18}$$

Thus, the summational invariants, ψ_1, ψ_2 and ψ_3, in the three preceding

cases under consideration, will assume the values,

$$\psi_1 = 1 \tag{19}$$

and

$$\psi_2 = m\vec{c} \tag{20}$$

$$\psi_3 = \frac{m\vec{c}^2}{2} \tag{21}$$

Having obtained the summational invariants as well as the relations between the VDF and macroscopic quantities of the flow, one can now solve the problem in a straight forward manner. With the aid of ψ_i's, it may be noted that the term,

$$\frac{\partial_e f}{\partial t}$$

describing the effect of particle encounters can be reduced to zero if it is multiplied by a summational invariant and integrated with respect to $\vec{c}$ in the velocity space. Thus multiplying each term in the Boltzmann Eq. (6) with the ψ_i's and integrating with respect to $\vec{c}$ in the velocity space, we have

$$\int \psi_i \; c \cdot \nabla_r f \, d\vec{c} + \int \psi_i \, \vec{F} \cdot \nabla_c f \, d\vec{c} = \int \psi_i \, \frac{\partial_e f}{\partial t} \, d\vec{c} \tag{22}$$

According to Eq. (18), the term on the right-hand side vanishes in all cases. By this method, the exact expression of

$$\frac{\partial_e f}{\partial t}$$

is therefore not needed, but the effect of particle encounters has properly been taken into account.

Inserting, successively, in Eq. (22) the three values of the summational invariants, ψ_1, ψ_2 and ψ_3, as given in Eqs. (19), (20) and (21), a set of three integral equations of the following form is obtained.

Case ψ_1:
$$\int \vec{c} \cdot \nabla_r f \, d\vec{c} + \int \vec{F} \cdot \nabla_c f \, d\vec{c} = 0 \tag{23}$$

Case ψ_1:
$$m \int \vec{c} \; \vec{c} \cdot \nabla_r f \, d\vec{c} + m \int \vec{c} \; \vec{F} \cdot \nabla_c f \, d\vec{c} = 0 \tag{24}$$

Case ψ_1:
$$\frac{m}{2} \int \vec{c}^2 \; \vec{c} \cdot \nabla_r f \, d\vec{c} \quad \frac{m}{2} \int \vec{c}^2 \, \vec{F} \cdot \nabla_c f \, d\vec{c} = 0 \tag{25}$$

With the aid of the four definitions of the zero, first, second and third moments of the VDF as given in Eqs. (7), (8), (11) and (14), and after some mathematical transformations (see Appendix I), the six integrals occurring in the set of equations above can be carried out:

$$\nabla (n\vec{c}) = 0 \tag{26}$$

$$\nabla \cdot (kn\Theta) - mn\,[\vec{F} - \bar{\vec{c}} \cdot (\nabla\bar{\vec{c}})] = 0 \tag{27}$$

$$\nabla \cdot [(\Sigma\frac{kn\Theta_i}{2})\vec{c}] + \vec{c} \cdot [\nabla \cdot (kn\Theta)] + kn\Theta \cdot (\nabla\vec{c}) - mn\vec{c} \cdot [\vec{F} - \bar{\vec{c}} \cdot (\nabla\bar{\vec{c}})] = 0 \tag{28}$$

It may be noted in the set of the foregoing equations that "carrying out" the integrals was essentially replacing the microscopical quantities, $\vec{r}$, $\vec{c}$, $f(\vec{r},\vec{c})$ by a set of macroscopically definable mean values, viz., $\vec{F}$, n, $\bar{\vec{c}}$ and Θ. Their connection with the microscopical quantities was established in the definition of the different moments. It is in this step of the development that one loses the microscopic view and gains the macroscopic observation.

The physical content of Eqs. (26), (27) and (28) can easily be realized. Equation (26) is the familiar equation of conservation of charge and matter. Equation (27) is known as the equation of motion in the hydrodynamics of perfect fluids. The third equation, Eq. (28), essentially expressing the conservation of energy in the flow, is the new bit of information which is obtained by adopting the more general viewpoint of an existing temperature tensor Θ in the flow. The classical viewpoint is obtained at once, if the terms involving Θ are neglected. If Θ is put to zero, Eq. (28) reduces to Eq. (27) which in losing its term

$$\nabla \cdot (kn\Theta)$$

would precisely become the classical Eq. (2) mentioned in the introduction.

In other words, in the classical case the problem was attacked by solving Poisson's equation with the aid of the energy equation and the relation between current, charge and voltage. Turning our attention back to Eqs. (26), (27) and (28) which express the more general viewpoint adopted in this paper, one may note, that up to this point only three equations are at our disposal, whereas four macroscopic quantities, $\vec{F}$, n, $\bar{\vec{c}}$ and Θ are expected to be computed. Since Poisson's equation

correlates two of the four macroscopic quantities under consideration,

$$\nabla \cdot \vec{F} = 4\pi \frac{e^2}{m} n, \qquad (29)$$

viz., $\vec{F}$ and n, and is independent of the three equations mentioned above, it can be used as the necessary fourth equation to solve for the four macroscopic quantities, $\vec{F}$, n $\overline{\overline{c}}$ and Θ.

A brief summary of this chapter on the problem and its solution may be appropriate. The problem consists of solving Boltzmann's equation for the steady state case and for rectilinear flow, taking an integral effect of encounters into consideration. Solving Boltzmann's equation means, in the usual sense, solving for VDF under the particular conditions of the flow under consideration. But with the aid of four definitorial equations for the zero, first, second and third moments, a class of VDF's could be defined which may contain the "true function" and where any representative member of this class would approach any other member of this class of functions up to the third moment. With the knowledge of the overall behavior of a group of particles engaged in mutual encounters, expressed by the three summational invariants, three partial differential equations could be derived, connecting four macroscopic quantities, $\vec{F}$, n, $\vec{c}$ and Θ. With the additional information with respect to distributed space charges expressed by Poisson's equation, a set of four mutually independent equations is obtained, which represents the ultimate amount of information obtainable in describing the physical properties of the electron flow from this general viewpoint. It can be seen easily that these four equations are not yet sufficient to solve for the four macroscopic quantities under consideration. The reason is, of course, that the four equations are written in vector form and represent in the case of rectilinear flow a set of four scalar equations, since $\vec{F}$ and $\overline{\overline{c}}$ in Eq. (27) are parallel to each other. The number of unknowns, however, is six, since Θ has three components. Thus, two more conditions must be established to furnish the set sufficient for determining completely the desired macroscopic quantities. These two additional conditions can be considered as particular specifications of the problem. Two such problems, as it was indicated in the introduction, namely, the isotropic flow and the anisotropic flow, will be separately treated in the next section.

Before concluding this section on the problem and the method of its solution, it may be pertinent at this time to give a representative

function for the class of VDF's which may contain the "true function" as one of its members. Considering that any VDF selected should be consistent with the Eqs. (8), (11) and (14), which define the first, second and third moments, one may suggest, for example, a function of the form,

$$\varphi(\vec{u}) = n\left(\frac{m}{2\pi k}\right)^{3/2}(\Theta_1\Theta_2\Theta_3)^{-1/2}\exp\left[-\frac{m}{2k}\left(\frac{u_1^2}{\Theta_1}+\frac{u_2^2}{\Theta_2}+\frac{u_3^2}{\Theta_3}\right)\right] \qquad (30)$$

where n and Θ's may be functions of $\vec{r}$. This function is generally known as Schwarzschild's law[8] of ellipsoidal distribution of velocities.

III TWO ESSENTIAL TYPES OF FLOW

In the preceding section, it was pointed out that two more conditions are necessary for the complete determination of the six macroscopic quantities, $\vec{F}$, n, $\bar{\bar{c}}$, Θ_1, Θ_2 and Θ_3. In searching for the two conditions in question, one may explore certain specifications of the general problem, which should be appropriate for the actual situation under consideration. For example, imagine a situation in which the group of particles under consideration during their life time in the diode may have sufficient time to complete their mutual interactions. If it is possible to give a reasonable estimate of the time required to complete the mutual interaction, which may be called *relaxation time* t_R, then this situation is indeed realized if the transit time t_T for those particles is much longer than the "relaxation time" t_R. The statement above, that the group of electrons is allowed sufficient time to "complete their mutual interactions" means, of course, that this group has reached its equilibrium condition. From this, one can immediately infer that the three temperature components, Θ_1, Θ_2, Θ_3, for this particular group of electrons should be equal to each other. Hence, a situation as described above may be properly defined by:

$$\Theta_1 = \Theta_2 = \Theta_3 \tag{31}$$

Since all three temperature components in this case degenerate to one temperature scalar, this type of flow may be called the "isotropic flow". In our search for two more conditions essential in solving for the six macroscopic quantities, $\vec{F}$, n, $\bar{\bar{c}}$, Θ_1, Θ_2, Θ_3, one may note, with the aid of the set of four fundamental differential equations (26) - (29), that the specification as described above furnishes exactly the two necessary conditions over Eq. (31). Thus a necessary and sufficient set of equations has been established in order to determine completely the macroscopic quantities under consideration.

Similarly, imagine a situation in which the group of electrons emitted from the cathode are so swiftly drawn to the anode that no appreciable amount of particle encounters can take place in the space of the diode. This situation is realized if the transit time t_T for those electrons is much shorter than the relaxation time t_R for this particular group. Obviously, in this situation, the group of particles under consideration will not reach their equilibrium condition. However, an

observer, moving with the mean velocity along the electron flow, should in this case not be able to observe any essential change of the electron velocity distribution in the velocity components perpendicular to the axis of the flow. Thus the temperature components perpendicular to the direction of the flow become constant in the space interval of consideration. Hence, a situation as described above may be defined by:

$$\frac{\partial \Theta_2}{\partial x_1} = \frac{\partial \Theta_3}{\partial x_1} = 0 \tag{32}$$

Since all three temperature components in this case do not necessarily degenerate to one temperature scalar, this type of flow may be called the "anisotropic flow". One may note that the specification as described above again furnishes exactly two more necessary conditions in solving for our macroscopic quantities. Thus, in this case too, a necessary and sufficient set of equations has been established in order to determine completely the macroscopic quantities under consideration. The two situations briefly described above, namely the "isotropic flow" and the "anisotropic flow", will be separately discussed in two later paragraphs.

Now, we will turn our attention to a more precise determination of the two terms already discussed, viz., the "relaxation time", t_T, and the "transit time", t_R. In making a reasonable estimate of the time required for a group of particles to complete their mutual interactions, we shall follow essentially Chandrasekhar's extensive work[9] on the problem of encounters in stellar systems. The analogy with the electron gas is rather obvious if one considers that in both cases the interaction forces drop with the inverse square of the mutual distances of the particles in question. Chandrasekhar defines a relaxation time for a star cloud at that time: most of the particles need to alter, through the process of their mutual interactions, their original kinetic energy by about an equal amount. Accepting this definition and converting the quantities designed to fit the stellar case into quantities appropriate for the electron gas, one finds for the so determined relaxation time,

$$t_R = \frac{9}{16\sqrt{\pi}} \frac{\sqrt{m}\ (k\Theta)^{3/2}}{ne^4 \ln \frac{3k\Theta}{2e^2 n^{1/3}}} \tag{33}$$

With expression (33) for the "relaxation time", one can evaluate another quantity of interest, namely, the "mean free path". It may seem improper to define a mean free path for the electron gas. Nevertheless, it is instructive to define a length

$$\lambda = t_R \left(\frac{8k\Theta}{\pi m}\right)^{\frac{1}{2}} \tag{34}$$

which plays the same role for non-uniform electron gases as the mean free path does in the classical kinetic theory of gases, where the molecules are idealized as rigid elastic spheres. Of course, this "mean free path" is defined in the moving coordinate system and is applicable whether the gas as a whole is actually moving or not.

Having obtained an expression of the "relaxation time" for the group of particles under consideration, one may now determine the transit time for this group of particles. Since the transit time for a group of particles in a diode is nothing more than the mean life time of this group in a spatial interval an appropriate definition of what we may call a "mean transit time" may be given by

$$t_T = \int_a^b \frac{dx_1}{\bar{\bar{c}}\ (x_1)} \tag{35}$$

for a spatial interval between points a and b in which the electron gas is under consideration. Since the mean velocity, $\bar{\bar{c}}$, is a single-valued function of x_1, formula (35) is applicable to the entire region of the diodic flow. Without the definition of the mean velocity (Eq. (8)), one cannot define the transit time of electrons in all cases, especially of the emitted electrons which are eventually returned to the cathode.

The fundamental distinction between the two situations described above -- the isotropic and the anisotropic flow -- is that for isotropism, the relaxation time $(t_R)_{is}$ is very short in comparison with the transit time t_T

$$(t_R)_{is} << t_T$$

whereas for anisotropism, the relaxation time $(t_R)_{an}$ should be much longer than the transit time t_T

$$(t_R)_{an} >> t_T$$

This allows one to draw an important conclusion with respect to the

number density in both cases, since t_R is about inversely proportional to the number density of the electrons under consideration (see Eq. (33)). Assuming the transit time t_T for both cases to be roughly the same, the two cases may also be distinguished by the inequality

$$(t_R)_{an} > > > (t_R)_{is}$$

or using Eq. (33), which expresses the relaxation time in terms of the parameters describing the electron gas under consideration, one finds

$$(n)_{an} < < < (n)_{is}$$

This strong inequality suggests that Poisson's equation will degenerate to Laplace's equation in the case of the anisotropic flow.

The specifications given for the two situations are based upon the determination of the "relaxation time" and the "mean transit time" of the group of particles in question. In concluding the introductory part of this section on the two essential types of flow, it might be well to list all the equations which will be used in solving the problem. However, for the sake of simplicity, we shall confine ourselves to the parallel plane diode. For the electron flow in the parallel plane diode where the variations of the macroscopic quantities, $\vec{F}$, n, $\overline{\vec{c}}$, Θ_1's are only in the direction of the flow, the general equations derived for the electron flow are reduced to simpler forms. The general equations (26)-(29) expressed in their reduced form, together with the conditions of the specifications as mentioned above, are listed as follows:

$$\frac{d}{dx}(nv) = 0 \tag{36}$$

$$\frac{d}{dx}(kn\Theta_1) - mn\left(F - v\frac{dv}{dx}\right) = 0 \tag{37}$$

$$\frac{d}{dx}\left[\frac{knv}{2}(3\Theta_1 + \Theta_2 + \Theta_3)\right] - mnv\left(F - v\frac{dv}{dx}\right) = 0 \tag{38}$$

In the case of the "isotropic flow",

$$\frac{d}{dx}F = 0 \tag{39a}$$

$$\frac{d}{dx}\Theta_2 = \frac{d}{dx}\Theta_3 = 0 \tag{40a}$$

In the case of the "isotropic flow",

$$\frac{d}{dx} F = 4\pi \frac{e^2}{m} n \tag{39b}$$

$$\Theta_1 = \Theta_2 = \Theta_3 \tag{40b}$$

where F, v and x are used instead of $\vec{F}$, $\bar{c}$ and x_1.

The problem now consists of solving simultaneously the set of the above equations, (36) - (40). For the electron flow, Eqs. (36) - (38) are valid in general. In the case of the anisotropic flow, Eqs. (39a) and (40a) are added, whereas in the case of the isotropic flow, Eqs. (39b) and (40b) are added. However, some insight can be gained immediately by integrating Eq. (36) with respect to x. Equation (36) now becomes

$$nv = j \tag{41}$$

where j is an integration constant of the equation. Since the displacement current is zero in the steady-state case, je becomes the actual electric current density in the diode circuit. Equation (41) gives the functional relationship between the number density n and the mean velocity v of the electrons in the flow.

Another possibility of establishing a functional relationship valuable for both cases would be to eliminate the external force F from Eqs. (37) and (38). Eliminating F from these equations and making use of Eq. (36), one obtains

$$\frac{d}{\Theta_1 dx} (\Theta_1 + \Theta_2 + \Theta_3) + \frac{2}{v} \frac{dv}{dx} = 0 \tag{42}$$

In the case of the "anisotropic flow" where the temperature components, Θ_2 and Θ_3, are independent of x, Eq. (42) yields

$$\Theta_1 (x) [v(x)]^2 = \Theta_1 (o) [v(o)]^2 = \text{constant} \tag{43}$$

where $\Theta_1(o)$ and v(o) are the x-component of the electron temperature and the mean velocity at the emission surface. The macroscopic quantities at the emission surface are known as boundary values, the evaluation of which will be given later. Similarly, in the case of the

"isotropic flow" where the components of the electron temperature are equal to each other, Eq. (42) then yields

$$[\Theta_1(x)]^3\ [v(x)]^2 = [\Theta_1(o)]^3\ [v(o)]^2 = \text{constant} \qquad (44)$$

These two equations indicate that the electron temperature in the electron flow of a parallel plane diode decreases as the mean velocity of the electrons increases (Appendix II). If one could find the mean velocity as a function of x in the electron flow under consideration, the variation of the electron temperature along with the electron flow could be determined from Eqs. (43) and (44).

In the following, we shall consider separately the two types of flow; first, the "anisotropic flow" and second, the "isotropic flow".

3.1 Anisotropic Flow

As mentioned before, the problem now is to solve simultaneously Eqs. (36), (37), (38), (39a), and (40a) for the case of the anisotropic flow. It is clear that the LaPlace equation, (39a), for the field between two parallel planes merely implies that

$$F = \frac{e}{m} E \qquad (45)$$

where E is the applied electric field, independent of the coordinate x. With Eq. (45) and the two functional relationships, Eqs. (41) and (43) just derived, one is able to replace n, Θ_1 and F of Eq. (37) in terms of the mean velocity v and the applied electric field E. Equation (37) then reads

$$v \frac{dv}{dx} - \frac{A}{v^3} \frac{dv}{dx} - \frac{eE}{m} = 0 \qquad (46)$$

where

$$A = \frac{3k\ \Theta_1\ (o)\ [v(o)]^2}{m}$$

Since $\Theta_1(o)$ and v(o) are the boundary values of the temperature component and the mean velocity of the flow, A is independent of the coordinate x. After the equation is integrated with respect to x, we have

$$v^2 + \frac{A}{v^2} - \frac{2eEx}{m} = G \qquad (47)$$

In this equation, G is an integration constant independent of x. Since

$$v = v(o) \qquad \text{at } x = o$$

one obtains from Eq. (47) that

$$G = v^2(o) + \frac{A}{v^2(o)}$$

With the constants A and G, determined as above, Eq. (47) can be written

$$\left\{\left[\frac{v(x)}{v(o)}\right]^2 - 1\right\} - \frac{3k\,\Theta_1(o)}{m[v(o)]^2}\left\{1 - \left[\frac{v(o)}{v(x)}\right]^2\right\} = \frac{2eEx}{m[v(o)]^2} \qquad (48)$$

From the above equation, one may calculate the mean velocity v as a function of the coordinate x for an electric field E.

In order to expose the physical contents of Eq. (48), it is first necessary to show how the boundary values in the equation are determined. To do this, the surface condition of both cathode and anode has to be found. Although our understanding of the thermionic emission[10] has been advanced considerably in the last decade, we are still unable to calculate the quantities n, v and Θ_1 accurately at the emission surface. Here we use a reasonable model from which these values can be evaluated. The accepted model is as follows. All the electrons which arrive at the anode are collected by the anode without causing any stray disturbances. The emission surface can be simulated by a uniform surface of work function W with a velocity dependent transmission coefficient D of the simple form, Fig. 2, pg. 4. Based on Nottingham's experimental work[11], this is designed to approximate the actual coefficient by a simpler form in which the normal energy ϵ is of the order of half an electron volt. Then the VDF at the emission surface becomes

$$f(o) = \frac{2m^3}{h^3} D \exp\left[-\frac{eW}{kT}\right] \exp\left[-\frac{m(c_1^2 + c_2^2 + c_3^2)}{2kT}\right], \quad c_1 > 0 \qquad (49)$$

$$= 0 \qquad , \quad c_1 < 0$$

where T is the temperature of the emission surface. With this VDF at the emission surface, the boundary values n(o), v(o) and $\Theta_1(o)$ can be

evaluated in a straight forward manner (see Appendix III). The results are as follows:

$$n(o) = \frac{(2\pi\, mkT)^{3/2}}{2h^3} \left(\frac{kT}{e\epsilon}\right) \exp\left[-\frac{eW}{kT}\right] \tag{50}$$

$$v(o) = 2\left(\frac{2kT}{\pi m}\right)^{1/2} \left[1 - \exp\left(-\frac{eW}{kT}\right)\right] \tag{51}$$

$$\Theta_1(o) = \frac{3\pi - 8}{\pi}\, T \tag{52}$$

Having evaluated the boundary values as above, one can see that Eq. (48) is normalized by the mean velocity of the electrons at the emission surface. As compared with Eq. (2) of the single-valued velocity theory, Eq. (48) contains an additional term, the second term on the left-hand side of Eq. (48). Since the factor

$$\frac{3k\,\Theta_1(o)}{mv^2\ (o)}$$

in this term is usually of the order of unity, this additional term is actually a correction term to calculate the mean velocity of the electrons close to the emission surface. When the ratio

$$\frac{v(x)}{v(o)}$$

becomes large, the velocities calculated from Eq. (2) and Eq. (48) are about the same. After the mean velocity of the electrons in the diode is obtained, the number density and the electron temperature can easily be determined from the functional relationships derived before. In short, from Eqs. (41) and (43),

$$n(x) = n(o) \left[\frac{v(o)}{v(x)}\right] \tag{53}$$

and

$$\Theta_1(x) = \Theta(o) \left[\frac{v(o)}{v(x)}\right]^2 \tag{54}$$

As a conclusion, a typical example for the anisotropic flow may be cited here. Suppose the work function[12] of the emission surface is

1.2 volt; the values of t_R and λ (Fig. 3) are calculated from Eqs. (33) and (34) against the cathode temperature. In a case of operation where

cathode temperature = 700°K

cathode anode spacing = 0.5 cm

anode voltage with respect to the cathode = 300 volts

one obtains from Eq. (33)

$$t_R = 1.8 \times 10^{-7} \text{ seconds,}$$

but from Eq. (48) and Eq. (35)

$$t_T = 1.9 \times 10^{-9} \text{ second,}$$

The result that

$$t_T << t_R$$

agrees with the specification given to this type of flow.

3.2 Isotropic Flow

As pointed out earlier, the number density n is generally high in the isotropic flow. This may be due to a weak applied field which does not draw all the emitted electrons away quickly enough. Also, it may occur if the emission current is too high for the applied voltage on the anode. In either circumstance, electrons may be accumulated to a very high density in front of the cathode. So the problem in this type of flow would be to solve simultaneously Eqs. (36), (37), (38), (39b) and (40).

The processes of solving these equations are very similar to those used in the case of the anisotropic flow. In the first step, the Poisson's Eq. (39b) can be written as

$$\frac{dF}{dx} = 4\pi \frac{je^2}{mv} \tag{55}$$

after relation (41) between the number density n and the mean velocity v is used. In the second step, one may replace n and Θ_1 of Eq. (37) in terms of the mean velocity v through the two functional relationships,

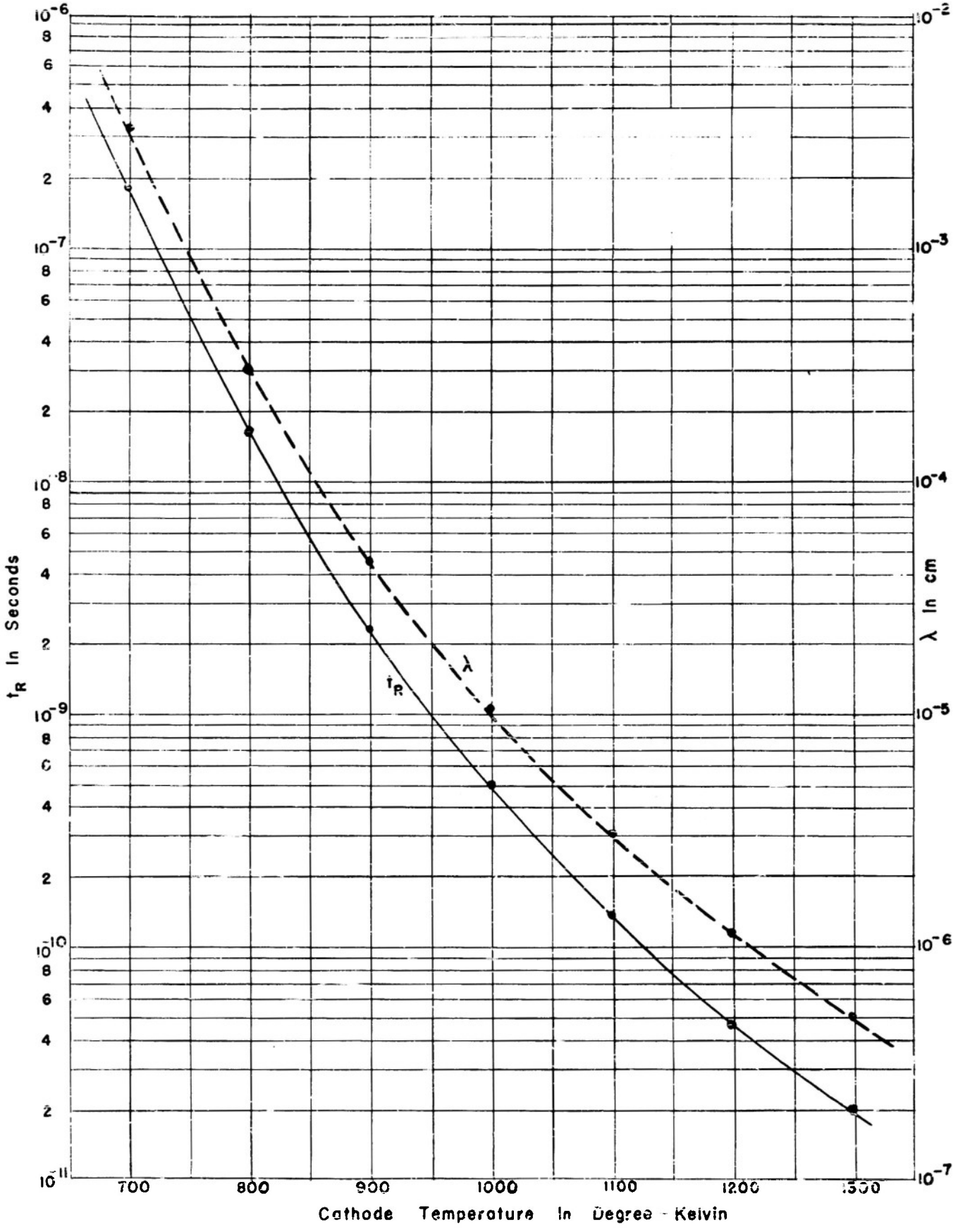

FIGURE 3 THE PLOT OF T_R AND λ CLOSE TO THE EMISSION SURFACE AGAINST THE CATHODE TEMPERATURE

Eqs. (41) and (44), derived before. Then,

$$v \frac{dv}{dx} - \frac{B}{v^{5/3}} \frac{dv}{dx} - F = 0 \tag{56}$$

where

$$B = \frac{5k\,\Theta_1\,(o)}{3m} [v(o)]^{2/3}$$

One may eliminate F from Eqs. (55) and (56) in order to obtain an equation for the mean velocity v for this type of flow. Differentiating Eq. (56) with respect to x and then combining it with Eq. (55) gives

$$(1 - \frac{B}{v^{8/3}})\, v \frac{d^2v}{dx^2} + (1 + \frac{5B}{3v^{8/3}}) (\frac{dv}{dx})^2 - \frac{4\pi je^2}{mv} = 0 \tag{57}$$

This equation does not involve the independent variable x explicitly[13] and it may therefore be reduced to a first-order linear differential equation by suitable transformations. The solution (see Appendix IV) can be written as

$$x + L = \int \left\{ M - \frac{8\pi je^2 v}{m}(1 + \frac{3B}{5v^{8/3}}) \right\}^{-1/2} (1 - \frac{B}{v^{8/3}}) v dv \tag{58}$$

This solution contains two integration constants, L and M, which have to be determined by two boundary conditions. It is clear that the non-constant force field, Eq. (39b), adds more difficulties in solving the problem for this type of flow.

Again, we shall use the reasonable model with which estimation of the boundary values can be made for the case of the isotropic flow. In doing this, it is obvious that the present method is by no means the most accurate, but certainly serves as an illustration of how boundary values in this problem may be determined.

In the isotropic flow the expression for the cathode emission

$$j_t = \frac{4\pi m}{h^3} (kT)^2 \frac{kT}{e\epsilon} \left\{ 1 - \exp\left[-\frac{e\delta}{kT}\right] \right\} \exp\left[-\frac{eW}{kT}\right] \tag{59}$$

remains the same; but a large portion of the emitted current is com-

pensated by the returning component of the current at the emission surface. Thus the actual current density, j, of the isotropic flow is one such that

$$\frac{j}{j_t} = R_S << 1 \tag{60}$$

This parameter R_S is the ratio of the number of electrons actually drawn to the anode and the number of emitted electrons per unit area in unit time. Hence R_S can be regarded as one of the operating conditions of the diode. In this situation, the electron gas at the emission surface would not follow the half-maxwellian VDF, Eq. (49), but rather approach a nearly symmetric maxwellian VDF. This nearly maxwellian electron gas may stretch itself out to a great extent away from the cathode. In other words, one can then assume the electron gas at the emission surface to be in equilibrium with the emitter,

$$\Theta_1(o) = T \tag{61}$$

Since the electron gas at the emission surface is nearly maxwellian, the returning component of current is

$$n(o)\left[\frac{kT}{2\pi m}\right]^{1/2}$$

With the above description of this model, the boundary values of n, v and Θ_1 can be determined at the cathode surface. They are:

$$n(o) = j_t(1 - R_S)\left[\frac{2\pi m}{kT}\right]^{1/2} \tag{62}$$

$$v(o) = \frac{R_S}{1 - R_S}\left[\frac{kT}{2\pi m}\right]^{1/2} \tag{63}$$

$$\Theta_1(o) = T \tag{64}$$

in which j_t, T and R_S are considered as known quantities.

To evaluate the two constants, L and M, in Eq. (58), another boundary value of the mean velocity v must be determined for this

problem. For this purpose one may consider that the number density of the electron flow decreases as the mean velocity increases in the flow. From the expression for the relaxation time, it is noticed that the relaxation time is about inversely proportional to the number density of the electrons under consideration. Because the condition of this type of flow is specified through the relaxation time, it is apparent that the isotropic flow may become anisotropic if the electrons in the flow are accelerated to reach sufficiently high velocities. In the region where the mean velocity reaches a sufficiently high value, the percentage difference of the mean velocities calculated from the Eqs. (47) and (58) for the two types of flow is much smaller than the difference in the region of low mean velocity. Because of this fact, a good approximate value of $v(x_2)$ can be calculated from Eq. (47) for the anisotropic flow, provided that a suitable distance x_2 is selected for the calculation. In the space-charge-limited flow, this distance x_2 may be longer than the actual cathode-anode spacing and is used only for the purpose of determining the second boundary value of the mean velocity in the flow.

The boundary values of the mean velocity at a distance t_2 and at the cathode surface are necessary and sufficient to evaluate the constants, L and M, in Eq. (58). After evaluating these constants, one can calculate the mean velocity v(x) throughout the isotropic flow. Using the same manner as for the anisotropic flow, one can also find that

$$n(x) = n(o)\left[\frac{v(o)}{v(x)}\right] \tag{65}$$

and

$$\Theta_1(x) = \Theta_1(o)\left[\frac{v(o)}{v(x)}\right]^{2/3} \tag{66}$$

As a conclusion for this section, some calculated results may be cited here. Using the same example as given for the anisotropic flow, one may raise the cathode temperature to 1100°K. When the anode voltage is about 300 volts, the parameter R_S has the value of 0.005. From Eqs. (58) and (35), the mean transit time of the flow is obtained

$$t_T = 2.4 \times 10^{-8} \text{ second}$$

for an interval from v(o) to 10 v(o). However, from expression (33),

one may calculate the relaxation time in this case,

$$t_R = 3.4 \times 10^{-12} \text{ second}$$

The result that

$$t_R >> t_R$$

justifies the condition adopted to specify this type of flow.

APPENDIX I

DERIVATION OF THE FLOW EQUATIONS

In this appendix, the derivation of the flow equations, (26)-(28) is given in detail. This is provided as a review* for the convenience of the reader.

Multiplying each term in the Boltzmann Eq. (6) by ψ and integrating with respect to $\vec{c}$ in the velocity space, one obtains

$$\int \psi \vec{c} \cdot \nabla_r f \, d\vec{c} + \int \psi \vec{F} \cdot \nabla_c f \, d\vec{c} = \int \psi \frac{\partial_e f}{\partial t} \, d\vec{c} \tag{22}$$

Using the rule of integration by parts, one can write

$$\int \psi c_1 \frac{\partial f}{\partial x_1} \, d\vec{c} = \frac{\partial}{\partial x_1} \int \psi c_1 f \, d\vec{c} - \int f c_1 \frac{\partial \psi}{\partial x_1} \, d\vec{c} = \frac{\partial n \overline{c_1}}{\partial x_1} - n \overline{c_1 \frac{\partial \psi}{\partial x_1}} \tag{I}$$

and

$$\int \psi \frac{\partial f}{\partial c_1} \, d\vec{c} = \iint [\psi f]_{c_1 = -\infty}^{c_1 = \infty} dc_2 dc_3 - \int f \frac{\partial \psi}{\partial c_1} \, d\vec{c} = -n \overline{\frac{\partial \psi}{\partial c_1}} \tag{II}$$

where $\vec{c}$ and $\vec{r}$ are separate independent variables of f, and $\vec{c}$ is independent of $\vec{r}$. Since the usual hypothesis is that ψf tends to zero as c_1 tends to infinity in either direction, the integrand in the second integral of Eq. (II) vanishes in general. If ψ denotes one of the summational invariants, the right-hand side of Eq. (22) vanishes in general. With expressions (I) and (II) available, Eq. (22) can be written in the following form:

$$\nabla_r \cdot n \overline{\psi \vec{c}} - n \left\{ \vec{c} \cdot \overrightarrow{\overrightarrow{\nabla_r \psi}} + \vec{F} \cdot \overrightarrow{\overrightarrow{\nabla_c \psi}} \right\} = 0 \tag{III}$$

It is more convenient to specify the VDF and ψ as functions not of $\vec{c}$ but $\vec{u}$, where

$$\vec{u} = \vec{c} - \bar{\vec{c}}$$

Hence, the next step is to express Eq. (III) in terms of the peculiar

*See for example S. Chapman and T.G. Cowling, *Mathematical Theory of Non-Uniform Gases*, Reference 6.

velocity $\vec{u}$. In changing the variable, we must replace

$$\overrightarrow{\nabla_c \psi} \qquad \text{by} \qquad \overrightarrow{\nabla_u \psi}$$

$$\frac{\partial \psi}{\partial x_i} \qquad \text{by} \qquad \frac{\partial \psi}{\partial x_i} - \frac{\partial \psi}{\partial u} \frac{\partial \bar{\vec{c}}}{\partial x_i}$$

and

$$\vec{c} \cdot \overrightarrow{\nabla_r \psi} \qquad \text{by} \qquad \vec{c} \cdot \overrightarrow{\nabla_r \psi} - \overrightarrow{\nabla_u \psi} \cdot (\vec{c} \cdot \nabla_r) \bar{\vec{c}}$$

One may note that the mean values are, of course, unaffected by the change of variable. After the substitutions of these terms, Eq. (III) becomes

$$\nabla_r \cdot n \overline{\psi(\bar{\vec{c}} + \vec{u})} - n \left\{ \overline{(\bar{\vec{c}} + \vec{u}) \cdot \overrightarrow{\nabla_r \psi}} - \overline{\overrightarrow{\nabla_u \psi} \cdot [(\bar{\vec{c}} + \vec{u}) \cdot \nabla_r] \bar{\vec{c}}} + \vec{F} \cdot \overline{\overrightarrow{\nabla_u \psi}} \right\} = 0 \tag{IV}$$

Making use of the identity

$$\overrightarrow{\nabla_u \psi} \cdot [\vec{u} \cdot \nabla_r] \bar{\vec{c}} \equiv \overrightarrow{\vec{u} \; \overrightarrow{\nabla_u \psi}} : \nabla_r \bar{\vec{c}}, \tag{V}$$

one can reduce Eq. (IV) to

$$\bar{\vec{c}} \cdot \nabla_r (n\bar{\psi}) + n \bar{\psi} \nabla_r \cdot \bar{\vec{c}} + \nabla_r \cdot n \overline{\psi \vec{u}}$$
$$- n \left\{ \bar{\vec{c}} \cdot \overrightarrow{\overrightarrow{\nabla_r \psi}} + \overrightarrow{\vec{u} \cdot \overrightarrow{\nabla_r \psi}} + (\vec{F} - \bar{\vec{c}} \cdot \nabla_r \bar{\vec{c}}) \cdot \overrightarrow{\overrightarrow{\nabla_u \psi}} - \overrightarrow{\vec{u} \overrightarrow{\nabla \psi}} : \nabla_r \bar{\vec{c}} \right\} = 0 \tag{VI}$$

The notation of two dots used in Eq. (V) is the so-called double product of two tensors. The significance of the bar placed over any quantity means the mean value of that quantity.

In the following, we shall consider Eq. (VI) for the three known values of summational invariants. For the case,

$$\psi_i = 1$$

then

$$\overline{\psi_1} = 1$$

$$\nabla_u \psi_1 = 0$$

$$\nabla_r \psi_1 = 0$$

Finally Eq. (VI) becomes

$$\nabla_r \, (n \, \overline{\vec{c}}) = 0 \tag{26}$$

For the case

$$\psi_2 = m \, (\vec{c} + \vec{u})$$

then

$$\overline{\psi_2} = m\overline{\vec{c}}$$

$$n\overline{\psi_2} \, \nabla_r \cdot \overline{\vec{c}} = mm\overline{\vec{c}} \cdot (\nabla_r \overline{\vec{c}})$$

$$n \, \overline{\psi_2 \vec{u}} = kn\Theta$$

$$\nabla_r \, \psi_2 = m \, \nabla_r \, \overline{\vec{c}}$$

$$\overline{\vec{u} \, \nabla_r \, \psi_2} = 0$$

$$\overline{\nabla_u \psi_2} = m$$

and

$$\overline{\nabla_u \, \psi_2 \, \vec{u}} = \overline{m\vec{u}} = 0$$

Hence, Eq. (VI) with the aid of Eq. (26), in this case, can be written

$$\nabla_r \cdot (kn \, \Theta) - mn \, [\vec{F} - \overline{\vec{c}} \cdot (\nabla_r \overline{\vec{c}})] = 0 \tag{27}$$

For the case,

$$\psi_3 = \frac{1}{2} m \, (\vec{u} + \overline{\vec{c}})^2$$

then

$$\overline{\psi_3} = \frac{1}{2} \, m\overline{\vec{c}}^2 + \sum_i k \, \Theta_i$$

$$n \, \overline{\psi_3 \vec{u}} = kn \, \Theta \cdot \overline{\vec{c}}$$

$$\overline{\nabla_r \psi_3} = \nabla_r \overline{\vec{c}}^2$$

$$\overline{u \nabla_r \psi_3} = k\Theta \cdot (\nabla_r \vec{c})$$

$$\nabla_u \psi_3 = \overline{m\vec{c}}$$

and

$$\overline{(\nabla_u \psi_3)\ \vec{u}} = k\ \Theta$$

With the aid of Eq. (26), Eq. (VI) can be reduced to

$$\nabla \cdot \left[(\Sigma \frac{kn\Theta_i}{2}) \overline{\vec{c}} \right] + \overline{\vec{c}} \cdot \left[\nabla \cdot (kn\Theta) \right] + kn\Theta \cdot (\nabla \overline{\vec{c}}) - mn\overline{\vec{c}} \cdot \left[\vec{F} - \overline{\vec{c}} \cdot (\nabla \overline{\vec{c}}) \right] = 0 \quad (28)$$

APPENDIX II
FUNCTIONAL RELATIONSHIP BETWEEN THE ELECTRON TEMPERATURE AND THE MEAN VELOCITY

In this appendix, we shall be concerned with the acquired knowledge of the variation of the electron temperature in a rectilinear flow. In the text, rectangular coordinates are chosen and the rectilinear flow is along the first coordinate, say x_1. In the case of the "anisotropic flow", we have

$$\frac{d}{dx_1}\ \Theta_2 = \frac{d}{dx_1}\ \Theta_3 = 0 \tag{40a}$$

and

$$\Theta_1\ v^2 = \text{constant} \tag{43}$$

Since the rectilinear flow is along the coordinate x_1, Eq. (40a) expresses the fact that the temperature components perpendicular to the flow Θ_2 and Θ_3, remain constant throughout the flow, whereas the temperature component along the flow Θ_1, decreases with the inverse square of the mean velocity v. (See Eq. (43)). In the case of the "isotropic flow",

$$\Theta_1 = \Theta_2 = \Theta_3 \tag{40b}$$

and

$$\Theta_1^3\ v^2 = \text{constant} \tag{44}$$

Since in this case the electron temperature components are equal to each other, Eqs. (40b) and (44) imply that all three temperature components will decrease with the inverse two-third power of the mean velocity.

In the above equations, the variation of the electron temperature is expressed in terms of the mean velocity in a rectilinear flow. In order to exhibit the functional relationships between the electron temperature and the mean velocity, it is worthwhile to plot the variations of the temperature components against the mean velocity on log-log paper. In such a plot they are straight lines as shown in Fig. 4.

In considering the velocity distribution of the electrons in the entire flow, it is necessary to study the variation of the temperature components in the velocity distribution function,

$$\varphi = n\left(\frac{m}{2\pi k}\right)^{3/2} (\Theta_1\ \Theta_2\ \Theta_3)^{-1/2} \exp\left[-\frac{m}{2k}\left(\frac{u_1^2}{\Theta_1} + \frac{u_2^2}{\Theta_2} + \frac{u_3^2}{\Theta_3}\right)\right]$$

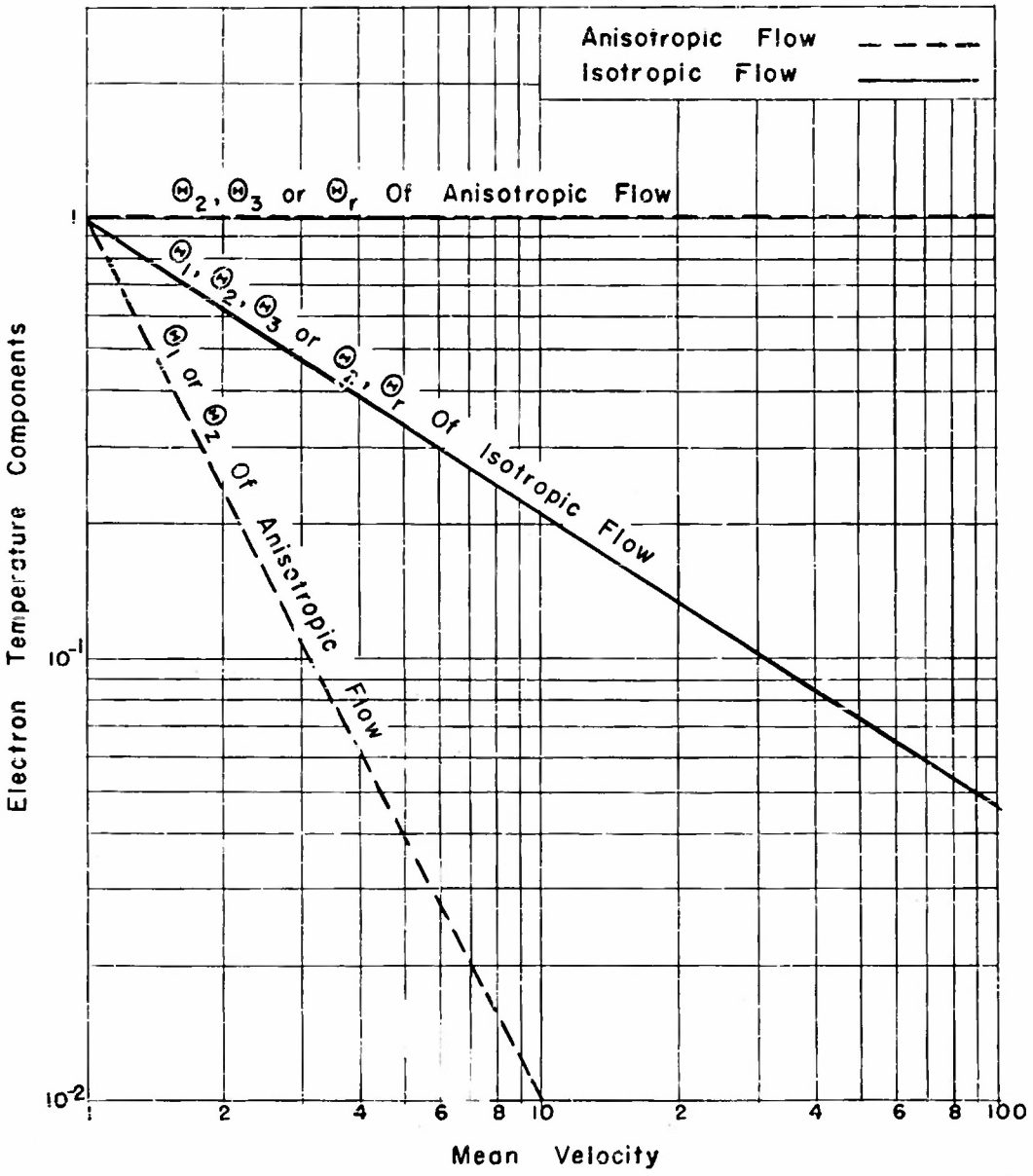

FIGURE 4 ELECTRON TEMPERATURE COMPONENTS VS. MEAN VELOCITY

If the rectilinear flow has a cylindrical symmetry, temperature components perpendicular to the flow are equal to each other. In this case, it is convenient to speak in terms of Θ_z instead of Θ_1, and Θ_r instead of Θ_2 and Θ_3. After this transformation, the velocity distribution function may be written

$$f = n\left(\frac{m}{2\pi k\Theta_r}\right)\left(\frac{m}{2\pi k\Theta_z}\right)^{1/2} \exp\left[-\frac{mc_r^2}{2k\Theta_r} - \frac{m(c_z - v)^2}{2k\Theta_z}\right]$$

One may note that, if the relationship between the mean velocity and the coordinate x along with the flow is established, the temperature components can be expressed as a function of x in the electron flow under consideration. If, for example, the Child-Langmuir law is accepted,

i.e., $$v \propto x^{2/3}$$

then the electron temperature becomes a defined function of the distance in the flow. Replacing v, the mean velocity, in Eqs. (43) and (44) by the Child-Langmuir relation, one obtains:

anisotropic flow: $$\Theta_1 \propto x^{-4/3}$$

and

$$\Theta_2 = \Theta_3 = \text{constant}$$

isotropic flow:

$$\Theta_i \propto x^{-4/9}, \quad i = 1, 2, 3.$$

These relations are plotted in Fig. 5

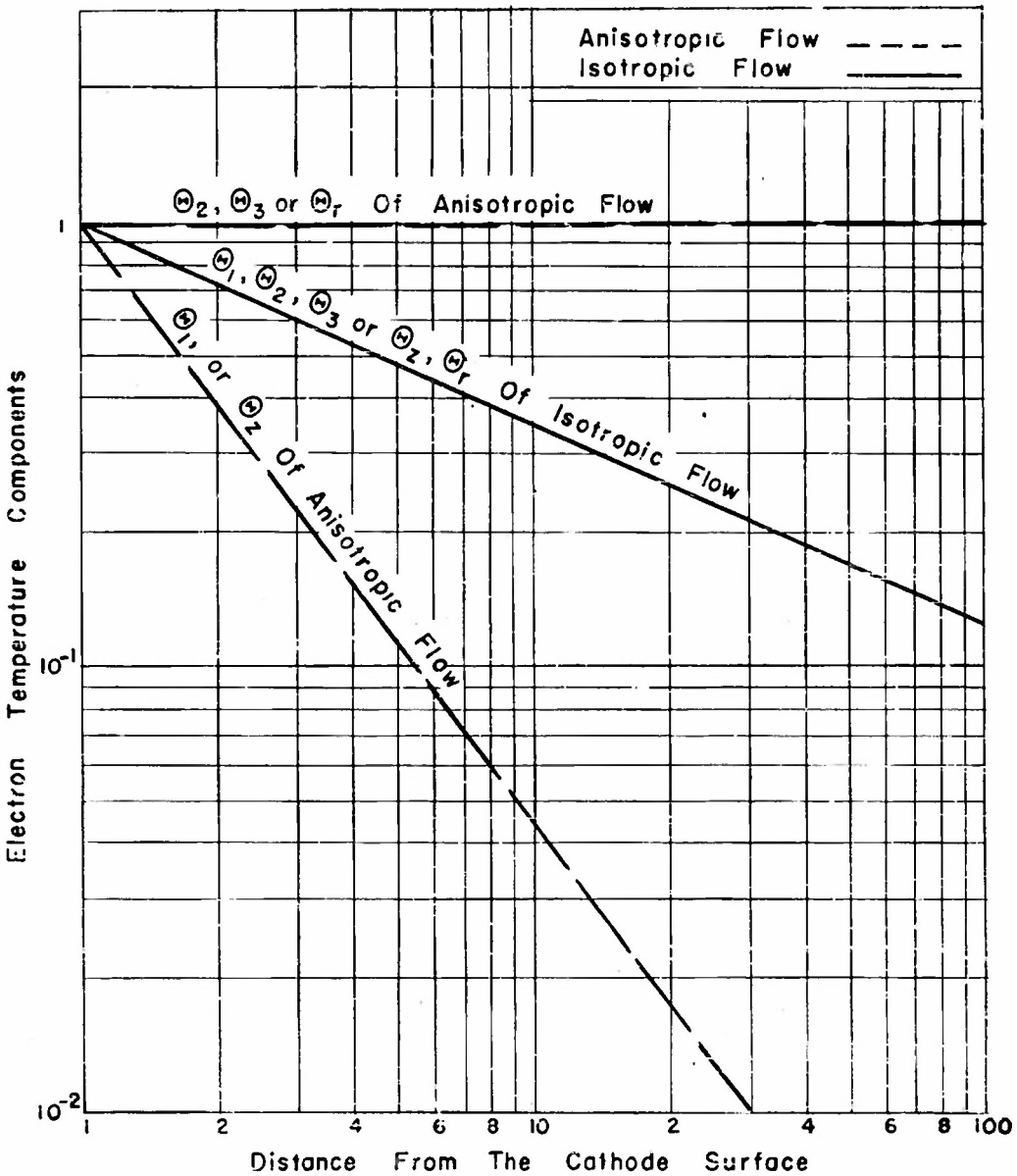

FIGURE 5 ELECTRON TEMPERATURE COMPONENTS VS. DISTANCE FROM THE CATHODE SURFACE

APPENDIX III
EVALUATION OF THE CONSTANTS AT THE EMISSION SURFACE

In this appendix, the calculations will be carried out under the assumption that at the emission surface the VDF is

$$f(o) = \frac{2m^3}{h^3} D \exp\left[-\frac{eW}{kT}\right] \exp\left[-\frac{m(c_1^2 + c_2^2 + c_3^2}{2kT}\right], \qquad c_1 > 0$$

$$= 0 \qquad , \qquad c_1 < 0$$

and the transmission coefficient D is

$$D = 1 \qquad \tfrac{1}{2} mc_1^2 \geq e\epsilon$$

$$= \frac{m c_1^2}{2e\delta} \qquad \tfrac{1}{2} mc_1^2 < e\epsilon$$

Let us first integrate the VDF with respect to c_2, c_3, i.e.,

$$\int_{c_2=-\infty}^{\infty} \int_{c_2=-\infty}^{\infty} f dc_1 dc_2 = \frac{2m^3}{h^3} \left(\frac{2\pi kT}{m}\right) D \exp\left[-\frac{eW}{kT}\right] \exp\left[-\frac{mc_1^2}{2kT}\right] \qquad \text{(VII)}$$

The integration with respect to c_1 is as follows:

$$\int_0^{(\frac{2e\epsilon}{m})^{\frac{1}{2}}} \frac{mc_1^2}{2e\delta} \exp\left[-\frac{mc_1^2}{2kT}\right] dc_1 + \int_{(\frac{2e\epsilon}{m})^{\frac{1}{2}}}^{\infty} \exp\left[-\frac{mc_1^2}{2kT}\right] dc_1 \qquad \text{(VIII)}$$

$$= -\frac{kT}{2e\delta} \left\{ c_1 \exp\left[\frac{mc_1^2}{2kT}\right] \Bigg|_0^{(\frac{2e\epsilon}{m})^{\frac{1}{2}}} - \int_0^{(\frac{2e\epsilon}{m})^{\frac{1}{2}}} \exp\left[-\frac{mc_1^2}{2kT}\right] dc_1 \right\}$$

$$+ \int_{(\frac{2e\epsilon}{m})^{\frac{1}{2}}}^{\infty} \exp\left[-\frac{mc_1^2}{2kT}\right] dc_1$$

With the transform

$$\frac{mc_1^2}{2kT} = y^2$$

and

$$dc_1 = \left(\frac{2kT}{m}\right)^{1/2} dy$$

expression (VIII) becomes

$$-\frac{kT}{(2me\delta)^{1/2}} \exp\left[-\frac{e\epsilon}{kT}\right] + \frac{(kT)^{3/2}}{(2m)^{1/2}e\delta} \int_0^{\left(\frac{e\epsilon}{kT}\right)^{1/2}} \exp\left[-y^2\right] dy + \left(\frac{2kT}{m}\right)^{1/2} \int_{\left(\frac{e\epsilon}{kT}\right)^{1/2}}^{\infty} \exp\left[-y^2\right] dy$$

Since ϵ is about 0.5 volt and kT is about 0.17 electron volt even at 2000°K, the value of $\left(\frac{e\epsilon}{kT}\right)$ is often much greater than unity. The third term has the same value but different sign as the first term, so only the second term is left to be evaluated. Expression VIII can therefore be approximated within an error of three percent by

$$\frac{kT}{2e\epsilon} \left(\frac{\pi kT}{2m}\right)^{1/2}$$

According to Eq. (7) in the text, one obtains from expressions (VII) and (VIII)

$$n(o) = \frac{(2\pi mkT)^{3/2}}{2h^3} \left(\frac{kT}{e\epsilon}\right) \exp\left[-\frac{eW}{kT}\right]$$

Second, J can be evaluated by first considering

$$\int_0^{\left(\frac{2e\epsilon}{m}\right)^{1/2}} \frac{mc_1^3}{2e\epsilon} \exp\left[-\frac{mc_1^2}{2kT}\right] dc_1 + \int_{\left(\frac{2e\epsilon}{m}\right)^{1/2}}^{\infty} c_1 \exp\left[-\frac{mc_1^2}{2kT}\right] dc_1$$

$$= -\frac{kTc_1^2}{2e\epsilon} \exp\left[-\frac{mc_1^2}{2kT}\right] \Bigg|_0^{\left(\frac{2e\epsilon}{m}\right)^{1/2}} - \frac{(kT)^2}{me\epsilon} \exp\left[-\frac{mc_1^2}{2kT}\right] \Bigg|_0^{\left(\frac{2e\epsilon}{m}\right)^{1/2}}$$

$$- \frac{kT}{m} \exp\left[-\frac{mc_1^2}{2kT}\right] \Bigg|_{\left(\frac{2e\epsilon}{m}\right)^{1/2}}^{\infty}$$

$$= \frac{(kT)^2}{me\delta}\left[1 - \exp\left[-\frac{e\epsilon}{kT}\right]\right]$$

According to Eq. (8) in the text, one then gets

$$J = \frac{4\pi m}{h^3}\frac{(kT)^3}{e\epsilon}\left[1 - \exp\left(-\frac{e\epsilon}{kT}\right)\right]\exp\left[-\frac{eW}{kT}\right]$$

and

$$v(o) = 2\left(\frac{2kT}{\pi m}\right)^{\frac{1}{2}}\left[1 - \exp\left(-\frac{e\epsilon}{kT}\right)\right]$$

Third, the following integrals are considered in evaluating the temperature component Θ_1 at the cathode surface:

$$\int_o^{(\frac{2e\epsilon}{m})^{\frac{1}{2}}} \frac{mc_1^2}{2e\delta}(c_1 - v)^2 \exp\left(-\frac{mc_1^2}{2kT}\right)dc_1 + \int_{(\frac{2e\epsilon}{m})^{\frac{1}{2}}}^{\infty}(c_1 - v)^2 \exp\left(-\frac{mc_1^2}{2kT}\right)dc_1 \qquad (IX)$$

Again, with the transform

$$\frac{mc_1^2}{2kT} = y^2$$

and

$$dc_1 = \left(\frac{2kT}{m}\right)^{\frac{1}{2}} dy$$

expression (IX) becomes

$$\int_0^{(\frac{e\epsilon}{kT})^{1/2}} (\frac{kT}{e\delta}) (\frac{2kT}{m})^{3/2} y^2 [y - (\frac{m}{2kT})^{1/2} v]^2 \exp [- y^2] dy + \int_{(\frac{e\epsilon}{kT})^{1/2}}^{\infty} (\frac{2kT}{m})^{3/2}$$

$$[y - (\frac{m}{2kT})^{1/2} v]^2 \exp [- y^2] dy$$

Since the value of $(\frac{e\epsilon}{kT})$ is often much greater than unity, the above expression may be approximated by

$$(\frac{kT}{e\delta}) (\frac{2kT}{m})^{3/2} \int_0^{\infty} y^2 [y - (\frac{m}{2kT})^{1/2} v]^2 \exp [- y^2] dy \qquad (X)$$

Using the known general integrals

$$\int_0^{\infty} y^{\gamma} \exp [- \alpha y^2] dy = - \frac{\sqrt{\pi}}{2} \cdot \frac{1}{2} \cdot \frac{3}{2} \cdot \frac{5}{2} \cdot \cdots \frac{\gamma - 1}{2} \alpha^{-(\gamma + 1)/2} \quad ; \quad \gamma = \text{even integer}$$

$$\int_0^{\infty} y^{\gamma} \exp [- \alpha y^2] dy = \frac{1}{2} \alpha^{-(\gamma + 1)/2} (\frac{\gamma - 1}{2})! \quad ; \quad \gamma = \text{odd integer}$$

and the expression of the mean velocity v evaluated above, Eq. (X), is reduced to

$$(\frac{3\pi - 8}{8\sqrt{\pi}}) (\frac{kT}{e\epsilon}) (\frac{2kT}{m})^{3/2}$$

According to the definition of Θ, Eq. (11), and the number density n evaluated above, one can simplify the expression so that

$$\Theta_1 = \frac{3\pi - 8}{\pi} T.$$

APPENDIX IV
SOLUTION OF THE EQUATION

$$\left(1 - \frac{B}{v^{8/3}}\right)v \frac{d^2v}{dx^2} + \left(1 + \frac{5B}{3u^{8/3}}\right) \left(\frac{dv}{dx}\right)^2 - \frac{4\pi je^2}{mv} = 0$$

The equation does not involve the independent variable x explicitly and it may therefore be reduced to a first-order differential equation by letting

$$\frac{dv}{dx} = y \qquad \text{and} \qquad \frac{d^2v}{dx^2} = y \frac{dy}{dv}$$

Then

$$\left(1 - \frac{B}{v^{8/3}}\right)vy \frac{dy}{dv} + \left(1 + \frac{5B}{3u^{8/3}}\right) y^2 - \frac{4\pi je^2}{mv} = 0$$

Furthermore, let

$$y^2 = z$$

then the above equation may be written as

$$\frac{dz}{dv} + \frac{2\left(1 + \frac{5B}{3v^{8/3}}\right)}{v\left(1 + \frac{B}{v^{8/3}}\right)} z = \frac{8\pi je^2}{mv^2\left(1 - \frac{B}{v^{8/3}}\right)}$$

This is a first-order linear differential equation, so it can be solved by the general method. First, evaluate the integral

$$\int \frac{2\left(1 + \frac{5B}{3v^{8/3}}\right)}{v\left(1 - \frac{B}{v^{8/3}}\right)} dv \qquad \text{(XI)}$$

It is more convenient if one uses

$$v^{8/3} = \omega \text{ and } dv = \frac{3}{8} \omega^{-5/3} d\omega$$

After this substitution, integral (XI) becomes

$$\int \frac{3}{4} \frac{\omega + \frac{5}{3} B}{\omega - B} \frac{d\omega}{\omega}$$

$$= \frac{3}{4} \int \frac{d\omega}{\omega} + 2B \int \frac{d\omega}{\omega(\omega - B)}$$

$$= \frac{3}{4} \ln \omega + 2 \ln \frac{\omega - B}{\omega}$$

$$= \ln \frac{(v^{8/3} - B)^2}{v^{10/3}}$$

Second, evaluate the integral

$$\int \frac{8\pi j e^2}{mv^2 (1 - \frac{B}{v^{8/3}})} \frac{(v^{8/3} - B)^2}{v^{10/3}} dv \qquad \text{(XII)}$$

$$= \frac{8\pi j e^2}{m} \int \frac{(v^{8/3} - B) v^{8/3}}{v^{16/3}} dv$$

$$= \frac{8\pi j e^2}{m} \left[\int dv - \int \frac{B\, dv}{v^{8/3}}\right]$$

$$= \frac{8\pi j e^2}{m} \left[v + \frac{3B}{5v^{5/3}}\right]$$

$$= \frac{8\pi j e^2 v}{m} \left[1 + \frac{3B}{5v^{8/3}}\right]$$

The solution of the linear equation can be written as

$$z = M \frac{v^{10/3}}{(v^{8/3} - B)^2} + \frac{8\pi je^2 v}{m} \left[1 + \frac{3B}{5v^{8/3}}\right] \left[\frac{v^{10/3}}{(v^{8/3} - B)^2}\right]$$

$$= \frac{v^{10/3}}{(v^{8/3} - B)^2} \left[M + \frac{8\pi je^2 v}{m} \left(1 + \frac{3B}{5v^{8/3}}\right)\right]$$

where M is an integration constant. So

$$\frac{dv}{dx} = \pm \frac{v^{5/3}}{(v^{8/3} - B)} \left[M + \frac{8\pi je^2 v}{m}\left(1 + \frac{3B}{5v^{8/3}}\right)\right]^{1/2}$$

If the positive sign is chosen, then

$$\frac{dx}{dv} = \frac{v^{5/3}}{v^{8/3} - B} \left[M + \frac{8\pi je^2 v}{m}\left(1 + \frac{3B}{5v^{8/3}}\right)\right]^{-1/2}$$

and

$$x + L = \int \left[M + \frac{8\pi jev}{m} \left(1 + \frac{3B}{5v^{8/3}}\right)\right]^{-1/2} \left(1 - \frac{B}{v^{8/3}}\right) v \, du$$

where L is another integration constant. It is clear that two boundary conditions are necessary in order to evaluate the integration constants, M and L.

PART II

DETERMINATION OF ELECTRON TEMPERATURE

1. INTRODUCTION

Ever since the discovery of thermionic emission, one-dimensional electron flow has been an interesting problem. The theory presented in Part I of this report deals with the electron gas in a rectilinear flow. In the theory, the electron flow between the cathode and the anode can be described completely with four macroscopic quantities:

1. External force field $\vec{F}$
2. Electron number density n
3. Mean velocity $\bar{\vec{c}}$
4. Electron temperature Θ

The first three quantities are familiar to us since they have been constantly used in the single-valued velocity theories. Experimental methods to determine these macroscopic quantities were developed long ago and are not discussed in this paper. However, the application of the last quantity, in this context the electron temperature tensor Θ, may be a constructive contribution in this field.

In Part II of this report, we shall devote ourselves to the development of a method which would enable us to measure the electron temperature in a rectilinear flow. Much of the attention will be given to the design of an apparatus with which the experiment is carried out. The present work is by no means a complete study of the subject, but the results of this experiment proved to be an interesting exposition concerning the temperature of the electron gas in a parallel plane diode.

2. THEORETICAL CONSIDERATIONS

In order to achieve the objectives stated in the introduction, theoretical consideration must first be given to the design of an apparatus which would be appropriate for the experiment to be performed. The apparatus should have an electron source, say, a cathode and an electrode acting as an anode to collect the arriving electrons. Since the electron flow discussed in Part I of this report is of rectilinear type, the structure of the apparatus is certainly expected to provide a parallel-plane flow between the cathode and the anode. In studying the velocity distribution of the electrons in the parallel-plane flow, use can be made of a field-free region. Ideally, one would take a sample of the electrons from the parallel-plane flow and set this sample of electrons free in a field-free region. The space distribution of the current in the field-free region would then exhibit the velocity distribution that the electrons had before they were set free. With the given definition of the electron temperature, an observed velocity spread can readily be expressed in terms of an electron temperature. This scheme would avoid the use of a probe usually applied in obtaining information at the point of interest. Here, in contrast to the probe measurements, the point of interest is placed at the boundary, hence there is no probe disturbance in the measurements. The most appropriate choice of a boundary would be the collector electrode. Thus, allowing a small sample of the flow to pass through an aperture into a field-free region would accomplish the desired function. With an arrangement of this sort in mind the essential feature of an apparatus can be sketched (Fig. 1). The apparatus consists of two parts, a parallel-plane diode and a field-free anode chamber. Although the detailed description of the apparatus will be given in the next section, its essential structure can be easily recognized. A small section of all the electrons forced in a Pierce arrangement to flow parallel from the cathode to the anode is permitted to enter a field-free region through a fine hole in the anode. Due to their radial velocity component, the thin beam will expand and the angular current-density distribution can be measured by again sampling a small section of that beam through a fine hole in a slide. As a result, the current-density distribution at the back wall of the anode chamber gives us the information about the velocity distribution of these electrons.

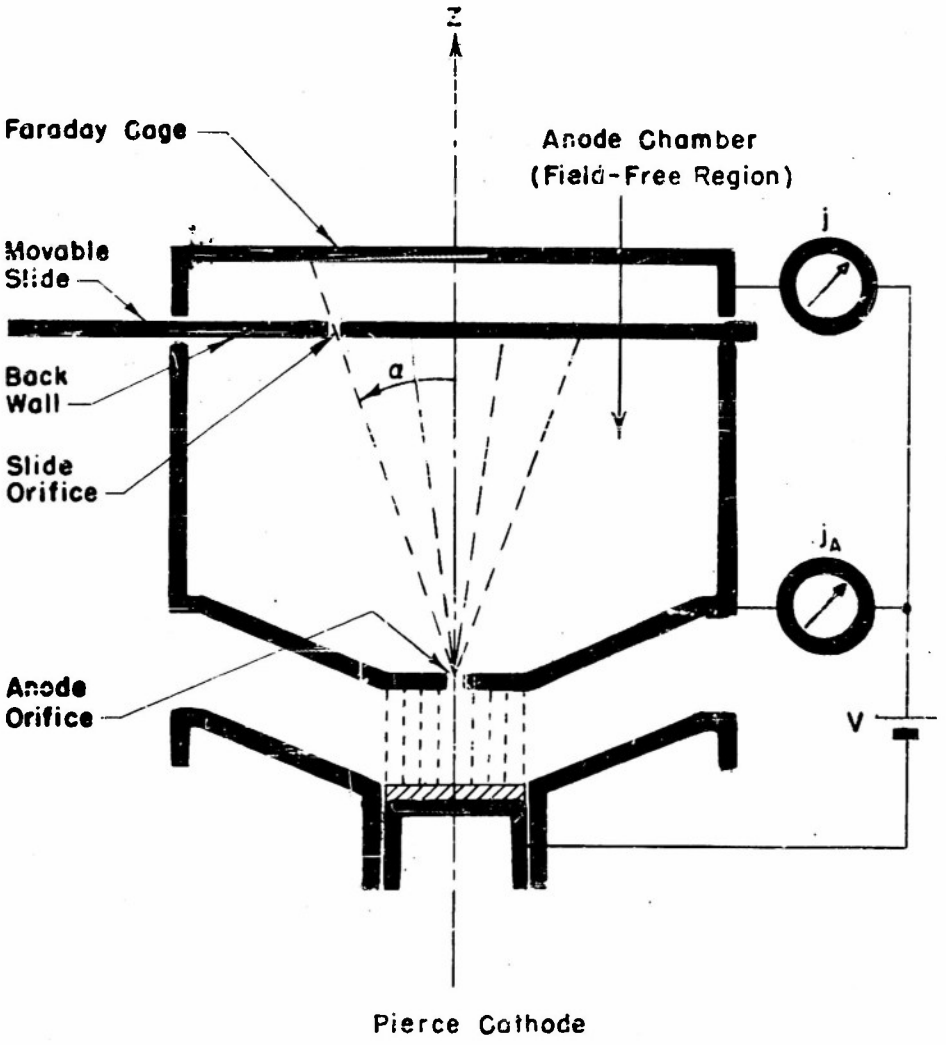

Radius of the Cathode	10 mm
Radius of the Anode Orifice	.17 mm
Radius of the Slide Orifice	.17 mm

FIGURE 1 SCHEMATIC DIAGRAM OF THE EXPERIMENTAL SETUP TO MEASURE THE RADIAL COMPONENT OF THE ELECTRON TEMPERATURE

In this experimental arrangement, deviations from the ideal case described above can be expected. They will be taken up in detail in a later section and will turn out to be very small indeed. In this section, however, we shall restrict ourselves to the calculation of the current-density distribution at the back wall of the anode chamber for the ideal case.

For this calculation, Fig. 2 is an illustrative diagram of the beam expansion due only to electron temperature. Anode plane is at z = 0; anode orifice is set at the origin. The back wall of the anode chamber is at z = Z.

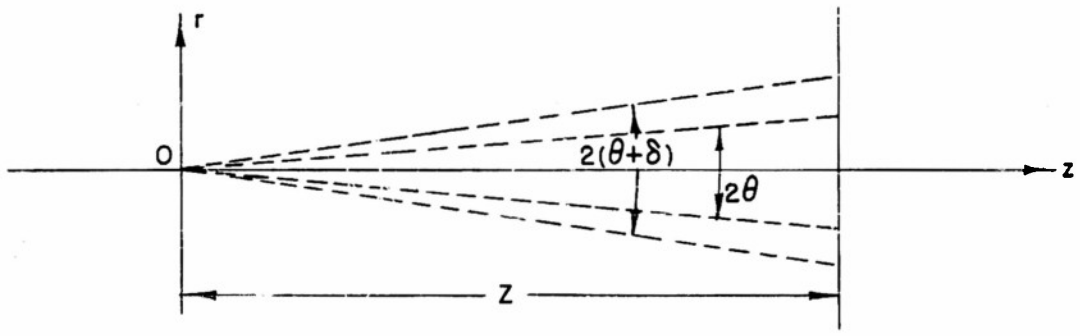

FIGURE 2 BEAM EXPANSION DUE TO ELECTRON TEMPERATURE

The calculation of the current-density distribution at the back wall of the anode chamber is based on the velocity distribution function dealt with in Part I of this report. From the point of view of the particle dynamics, the momentum and energy of the particles are the primary variables in the dynamic problems. Consequently, in practice one would not meet functions of the particle velocity higher than the quadratic term. As shown in Part I of this report, the moments higher than the third moment of the velocity distribution function do not appear in all the equations. Owing to this fact, one is able to select a representative VDF such as the one given in Eq. (30), Part I, of this report. It is noted that the given function is only a representative one in the class of the VDF's and will approach the "true function" up to the third moment. However, the VDF given in Eq. (30) is the appropriate one for the purpose and can be widely used in this field. Since

the structure of the apparatus will have a cylindrical symmetry, the VDF in Eq. (30) is now expressed with variables in the cylindrical coordinates, namely,

$$f = n \left(\frac{m}{2\pi k\Theta_r}\right) \left(\frac{m}{2\pi k\Theta_z}\right)^{1/2} \exp\left[-\frac{mc_r^2}{2k\Theta_r} - \frac{m(c_z - v)^2}{2k\Theta_z}\right] \tag{1}$$

where n is the number density, v is the mean velocity, Θ_r and Θ_z are the temperature components in the r and z directions of the electrons at the anode orifice.

With the velocity distribution function of Eq. (1), the calculation can be made in a straight-forward manner. Per unit area of the anode orifice, the current between the concentric cones with apex angles 2Θ and $2(\theta + \delta)$ as shown in Fig. 2 is

$$j(\theta,\delta) = n\left(\frac{m}{2\pi k\Theta_r}\right)\left(\frac{m}{2\pi k\Theta_z}\right)^{1/2} \int_0^\infty dc_z \int_{c_z \tan\theta}^{c_z \tan(\theta + \delta)} (c_z^2 + c_r^2)^{1/2} 2\pi\, d_r\, dc_r \cdot \exp\left\{-\frac{mc_r^2}{2k\Theta_r} - \frac{m(c_z - v)^2}{2k\,\Theta_z}\right\}$$

The above integration over C_z is carried from zero to infinity since only the electrons with a position velocity component in the z-direction will contribute to the current. Since the area of the anode orifice is πr_o^2, the current density of the Z-plane between the polar angles θ and $\theta + \delta$ becomes

$$J(\theta,\delta) = \frac{j(\theta,\delta)\pi r_o^2}{\pi Z^2 [\tan^2(\theta + \delta) - \tan^2\theta]}$$

Since the angle δ is small, C_r may then be approximated by $C_z \tan\theta$ under the radical sign. Ordinarily,

$$mv^2/2 > > k\Theta_r > k\Theta_z \tag{2}$$

so the above expression can be written as

$$J(\theta,\delta) = \frac{I_o}{\pi Z^2 \cos\theta}\left(1 + \frac{\Theta_z}{\Theta_r}\tan^2\theta\right)^{-3/2} \exp\left\{-\frac{mv^2}{2k\Theta_z}\left[1 - \left(1 - \frac{\Theta_z}{\Theta_r}\tan^2\theta\right)^{-1}\right]\right\} \cdot \frac{1 - \exp\left\{-\frac{mv^2}{2k\Theta_z}\left[\left(1 + \frac{\Theta_z}{\Theta_r}\tan^2\theta\right)^{-1} - \left(1 + \frac{\Theta_z}{\Theta_r}\tan^2(\theta+\delta)\right)^{-1}\right]\right\}}{\tan^2(\theta+\delta) - \tan^2\theta}$$

where I_o is the total current through the anode orifice,

$$I_o = nv\,\pi\, r_o^2$$

Because

$$\lim_{\delta \to 0} \frac{1 - \exp\left\{-\frac{mv^2}{2k\Theta_z}\left[\left(1 + \frac{\Theta_z}{\Theta_r}\tan^2\theta\right)^{-1} - \left(1 + \frac{\Theta_z}{\Theta_r}\tan^2(\theta+\delta)\right)^{-1}\right]\right\}}{\tan^2(\theta+\delta) - \tan^2\theta} = \frac{mv^2}{2k\Theta_r}$$

the expression of the current density at the Z-plane with a polar angle θ can be reduced to

$$J(\theta) = \frac{I_o}{\pi Z^2 \cos\theta}\left(1 + \frac{\Theta_z}{\Theta_r}\tan^2\theta\right)^{-3/2} \left(\frac{mv^2}{2k\Theta_r}\right) \exp\left\{-\frac{mv^2}{2k\Theta_z}\left[1 - \left(1 + \frac{\Theta_z}{\Theta_r}\tan^2\theta\right)^{-1}\right]\right\}$$

For small values of θ, this expression can be simplified to

$$J(\theta) = \frac{I_o}{\pi Z^2}\left(\frac{mv^2}{2k\Theta_r}\right) \exp\left\{-\frac{mv^2}{2k\Theta_r}\theta^2\right\} \qquad (3)$$

This current-density distribution at the Z-plane against the polar angle

is generally known as Normal or Gaussian law. It can also be written as:

$$\log_e \left[\frac{J(\theta)}{J(0)}\right] = -\eta\theta^2 \tag{4}$$

where

$$J(0) = \frac{I_o}{\pi Z^2}\,\eta$$

and

$$\eta = \frac{mv^2}{2k\Theta_r}$$

In this equation, $\log_e J(\theta)$ is a linear function of θ^2, and the slope of the straight line is η. Since Eq. (2) is valid in practice, it can be found from the flow equations in Part I of this report that

$$\tfrac{1}{2}\, mv^2 = eV \tag{5}$$

Therefore, the r-component electron temperature can be expressed as

$$k\Theta_r = \frac{eV}{\eta} \tag{6}$$

It may be noted that the beam radius at the Z-plane is large compared with the radius of the anode orifice. For high velocity beams, this Z-plane must be at a great distance from the anode. In this experimental set-up,

$$Z = 1.200 \text{ inch}$$

$$2r_o = 0.0135 \text{ inch}$$

then $Z/2r_o = 89$. In this case the beam diameter at the Z-plane is expected to be much larger than the diameter of the anode orifice. This justifies the consideration made in the calculation that the anode orifice can be regarded as a point source in this experimental arrangement. If the beam diameter at the Z-plane is not much larger than the diameter of the anode orifice, a correction has to be made for the finite size of the anode orifice.

3. EXPERIMENTAL APPARATUS

The diagram and the apparatus are shown in 3a and b. Essentially, the apparatus is a parallel plane diode (Fig. 1) which has cylindrical symmetry with respect to the z-axis. In this design, the anode is stationary and the cathode is movable. Anode, detector and a toroidal ring are all at the same potential V with respect to the cathode. A small orifice of 0.0135 in. diameter is provided at the center of the anode. The chamber behind the anode is almost closed and can be considered as a field-free region. Embedded in the back wall of the chamber is a running slide on which there is another small orifice of 0.0135 inch diameter. It is this orifice which acts as a movable opening on the back wall of the chamber.

A great effort has been made to have a parallel electron flow in the diode. When the cathode-anode spacing is small compared to the radius of the cathode, the electron flow close to the z-axis can be considered as parallel to the z-axis. It may be noted that the beam forming electrode is of the Pierce type, which is helpful in maintaining a parallel electron flow when the cathode-anode spacing and the potential difference V are increased. The potential on the beam forming electrode is so adjusted that the current to the toroidal ring is small or zero. The electron emitter is made heavier than the ordinary cathode sleeves to insure its flatness and to increase the heat capacity. An emission paste of half $BaCO_3$ and half $SrCO_3$ is used and the top of the emitter is electrophoretically coated with 4.4 mg/cm^2. The coated surface looks very homogeneous under the microscope.

Electrons which have emerged from the first orifice and also get through the second orifice will then be collected by the detector. The disturbances caused by the anode orifice will be considered in Section 4, as aberrations. When the disturbance is small, the electrons emerging from the anode orifice actually constitute a sample of the electrons arriving at the anode plane. In Section 4, it will also be shown that the flight of the electrons in the chamber is affected very little by the mutual repulsion force of the electrons. Therefore, the electrons having emerged from the anode orifice can be considered as flying through the chamber with their initial velocities at the anode.

As a result, the current density distribution on the back wall of the chamber is a direct consequence of the velocity distribution of

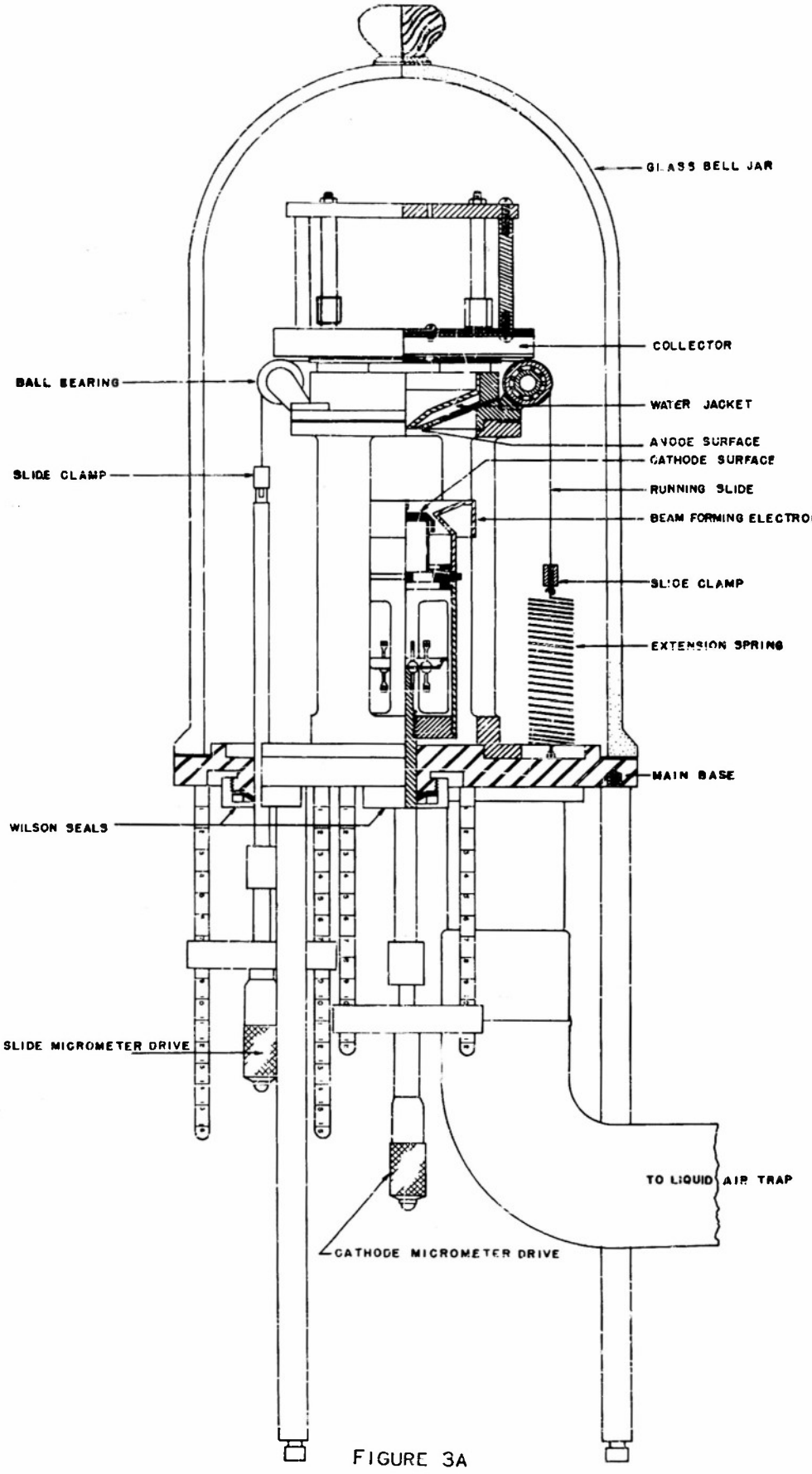

FIGURE 3A

R- COMPONENT TEMPERATURE ANALYZER

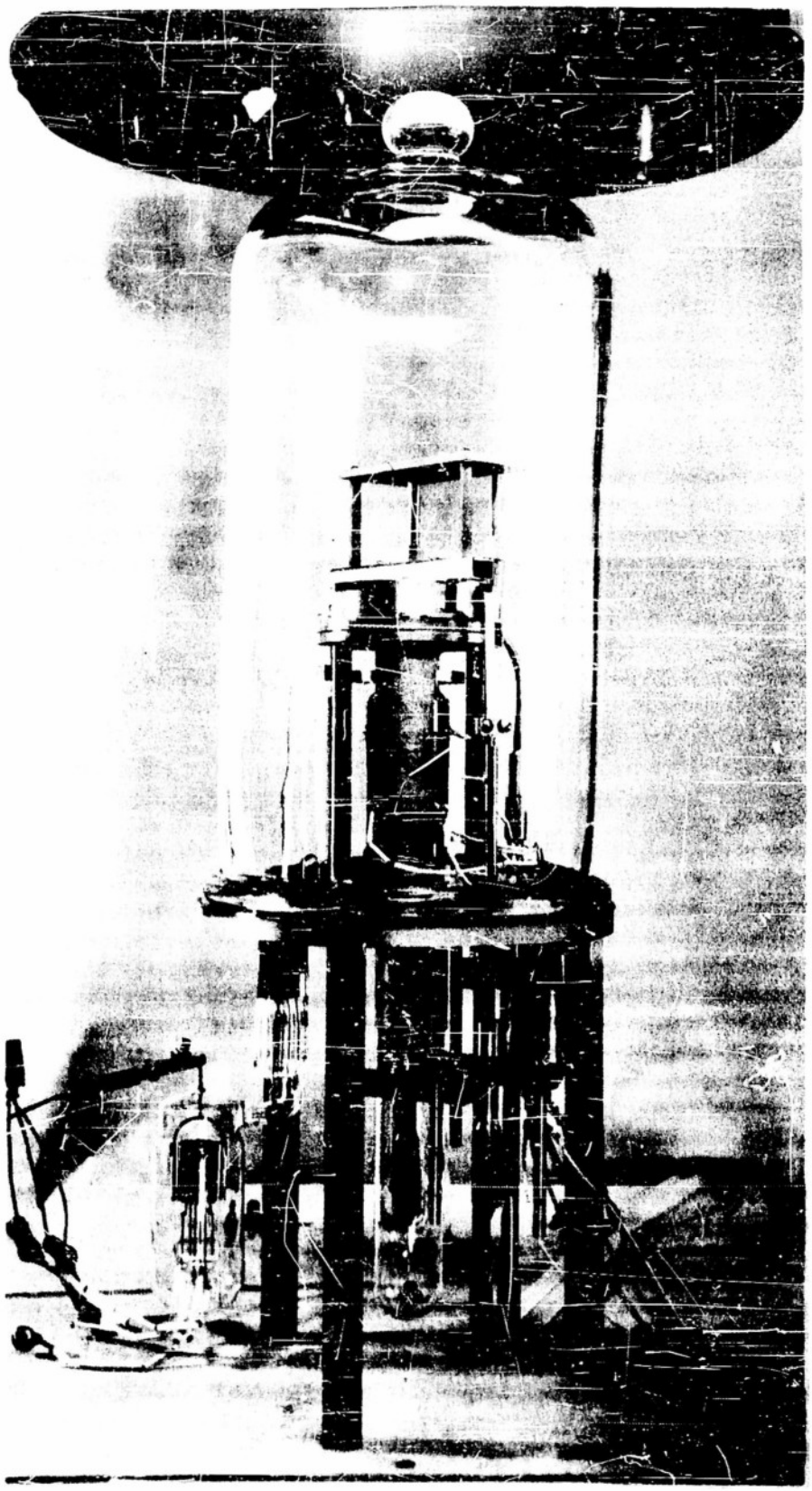

FIGURE 3B ASSEMBLY OF THE R-COMPONENT TEMPERATURE ANALYZER

electrons at the anode. The detector current indicates the current density at that point on the back wall of the chamber, at which the orifice of the running slide is set. By pulling the running slide, one may obtain the current density on the back wall as a function of r, the radial distance from the z-axis. From this information the electron temperature at the anode plane is evaluated.

Since the anode is supposed to collect all electrons which arrive at the anode without disturbing the electron flow, the electron flow in the various cathode-anode spacings can be considered the same as long as the same anode current is maintained by adjusting the anode voltage. When the same anode current is maintained, the anode plane can be placed at any distance from the cathode surface to determine the electron temperature at that plane. For one value of anode current, the electron temperature can then be determined as a function of the distance from the cathode surface.

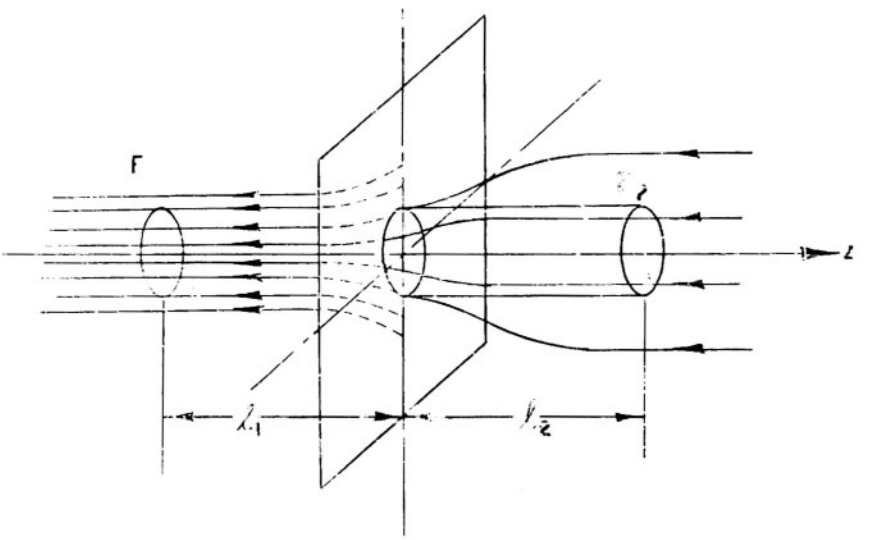

FIGURE 4 APPLICATION OF GAUSS' THEOREM TO A CIRCULAR APERTURE

4. ESTIMATION OF ABERRATIONS

As described in the preceding section, the apparatus is designed for the purpose of approaching the ideal case of the experiment. How good an approximation is attained can be seen in the study of the aberrations in this arrangement. It is conceivable that three kinds of aberrations would exist in the experiment. First, the presence of the anode orifice will cause an electron lens effect on the emerging beam; second, the emerging beam will undergo an expansion due to its space charge effect; third, the secondary electrons from the anode orifice will also give rise to a current-density distribution at the back wall of the anode chamber. Each of these effects will be estimated separately in the following three paragraphs.

4.1 Electron Lens Effect

The estimation of the divergent action of the anode orifice is made as if there were no velocity spread in the electron flow. Consider a cylinder (Fig. 4)*, symmetric with respect to z-axis, of cross-section area πr_o^2 and length $l_1 + l_2$, just long enough so that the electric fields across the ends of the cylinder are substantially uniform over the area. Thus, by Gauss' Theorem,

$$2\pi r_o \int_{-l_1}^{l_2} E_r(z)\, dz = -\pi r_o^2 (E_1 - E_2) - 4\pi^2 r_o^2 (l_1 + l_2) ne$$

or

$$\int_{-l_1}^{l_2} E_r(z)\, dz = -\frac{r_o}{2} (E_1 - E_2) - 2\pi r_o (l_1 + l_2) ne \qquad (7)$$

where n is the number density of electrons in the cylinder, E_1 and E_2 are the electric fields at the left and right ends of the cylinder, and E_r is the radial component of the electric field across the mantel surface of the cylinder.

Since the axial velocity of the electrons can be regarded as constant in the cylinder, the edge electrons will gain a radial component of velocity equal to

*See preceding page.

$$c_r = -\frac{e}{m}\int E_r\,dt = \frac{-\frac{e}{m}\int_{-l_1}^{l_2} E_r\,dz}{v} \tag{8}$$

In view of Eq. (7), the gain of the radial component of velocity is due to the additive result of two divergent actions: one comes from the change of electric field caused by the anode orifice, the other comes from the presence of space charge. The first action will be treated as an electron lens effect[14]; the second action as a space charge effect.

To estimate the electron lens effect, one must obtain an expression for the radial velocity. From Eq. (8)

$$c_r = \frac{e r_o (E_1 - E_2)}{2mv} \tag{9}$$

More explicitly, each electron entering the left end of the cylinder has the same velocity as given in Eq. (5) in the direction of the z-axis. Passing through the region of the cylinder, each electron will gain a radial component velocity as given in Eq. (9). Then their ratio will be

$$\frac{c_r}{v} = \frac{r_o (E_1 - E_2)}{4V}$$

where E_1, in a space charge limited diode, is

$$E_1 = \frac{4V}{3D}$$

and E_2, in the anode chamber, is

$$E_2 = 0$$

To describe the electron lens effect, we may best express the effect in terms of a polar angle θ_1 (at the center of the orifice) which the cross-sectional area of the beam at the back wall would subtend. In doing so, we have

$$\theta_1 = \arctan \frac{r_o}{3D} \left(1 + \frac{3D}{Z}\right) \tag{10}$$

In Fig. 6, this polar angle θ_1 is plotted against $\frac{D}{r_o}$. It should be noted that the electron path depends only upon the shape of the potential field and not upon the magnitude of the potential. As long as the configuration is maintained, the change of the anode potential should not cause any change of the deflection angle.

4.2 Space Charge Effect

Based on the analysis given by Spangenberg[15], one can also estimate the beam spread due only to space charge effect. For the purpose of analysis, it is convenient to start at a point where the radial velocity of the electrons can be considered zero. Assumed conditions are:

a. Electrons in the beam are distributed in a rotational symmetry with respect to the z-axis,

b. The axial velocity of the electrons in the beam remains the same in the consideration.

The analysis was primarily developed for high velocity electron beams. If there were no velocity spread in the electron flow, the beam spread thus predicted for the case of low velocity electron beams should still be reasonably accurate.

When the diode (Fig. 5) is space-charge-limited, the following relation exists:

$$\left(\frac{2}{9}\right)^{1/2} \frac{Z}{D} = \int_1^{\gamma} \frac{d\gamma}{(\log_e \gamma)^{1/2}} \tag{11}$$

where $\gamma = \frac{r}{r_o}$, r is the radius of the electron beam at position Z, and r_o is its radius at the orifice. Although Eq. (11) cannot be expressed in terms of elementary functions, it is clear that the percentage increase in the beam radius depends only upon the ratio of Z and D. Since r_o and Z are known in this experiment, Eq. (11), for the convenience of indicating the functional relationship, can also be written

$$\gamma = \gamma (D/r_o)$$

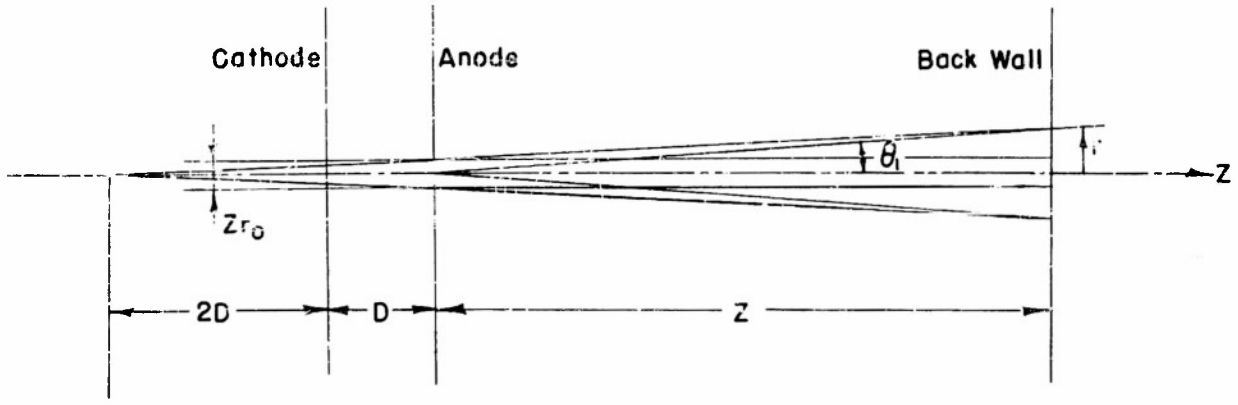

FIGURE 5 DIVERGENT ACTION OF A SINGLE APERTURE

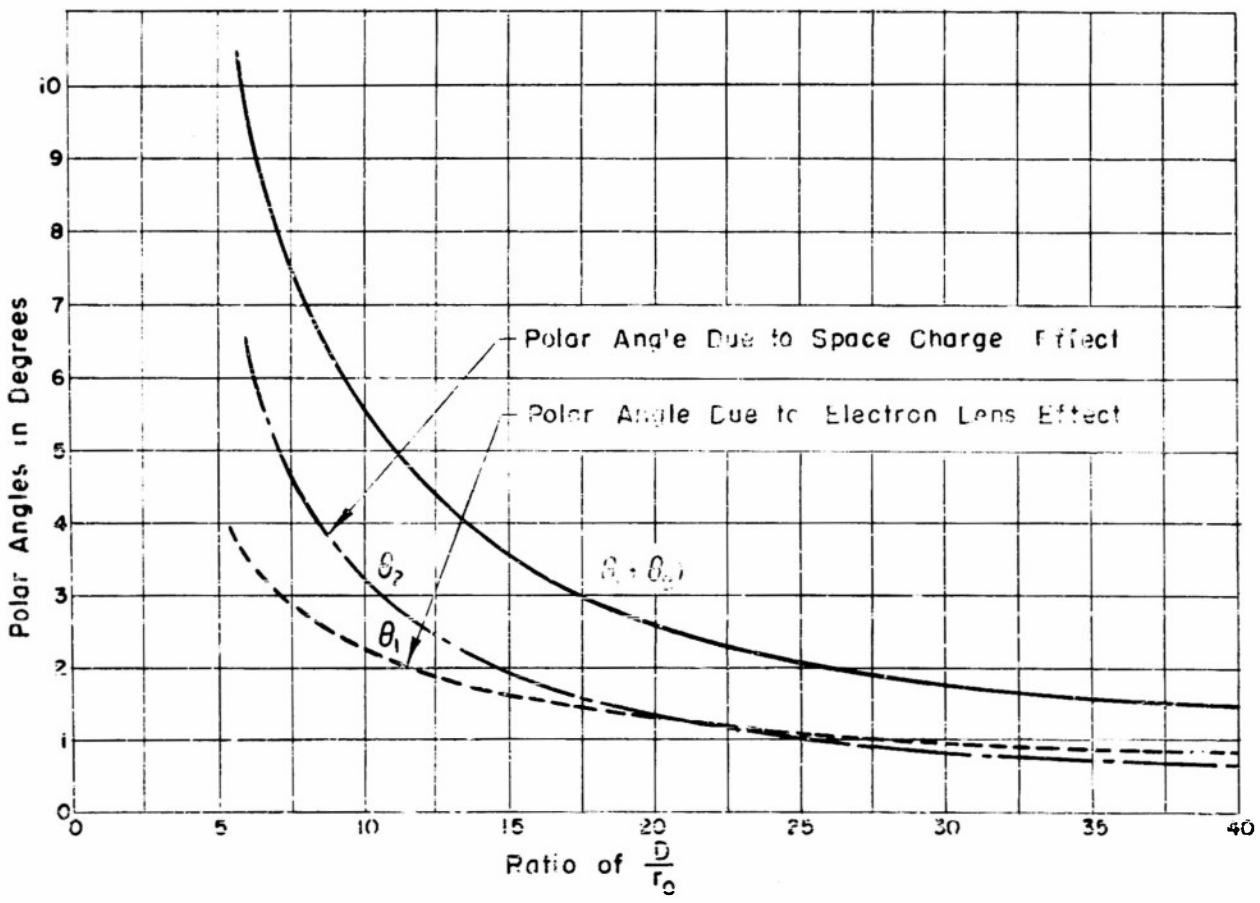

FIGURE 6 POLAR ANGLES AS A FUNCTION OF THE RATIO D/R_0

Putting the space charge effect on the same basis for comparison, we have

$$\theta_2 = \arctan \frac{r_o Y}{Z}$$

In Fig. 6, this polar angle θ_2 is also plotted against D/r_o. If the diode is in space-charge-limited operation, the beam expansion due to the space charge effect is also independent of the anode potential.

From Eqs. (7), (8) and (11), the radial velocity that an electron would gain before reaching the back wall is the sum of the velocities due to the electron lens effect and those due to the space charge effect. In Fig. 6, the sum of the polar angles, θ_1 and θ_2, is also plotted against D/r_o. Because

$$\tan \theta_1 + \tan \theta_2 \leq \tan (\theta_1 + \theta_2), \quad (\theta_1 + \theta_2) < 90°$$

$(\theta_1 + \theta_2)$ is a maximum polar angle estimated for the beam expansion in this experiment.

4.3 Secondary Electron Effect

In order to examine the effect of secondary electrons produced at the anode orifice, we shall calculate the current-density distribution at the back wall of the anode chamber due to the secondary electrons alone. In this calculation, the emitted secondaries are considered to enter the field-free region with negligible mutual interactions.

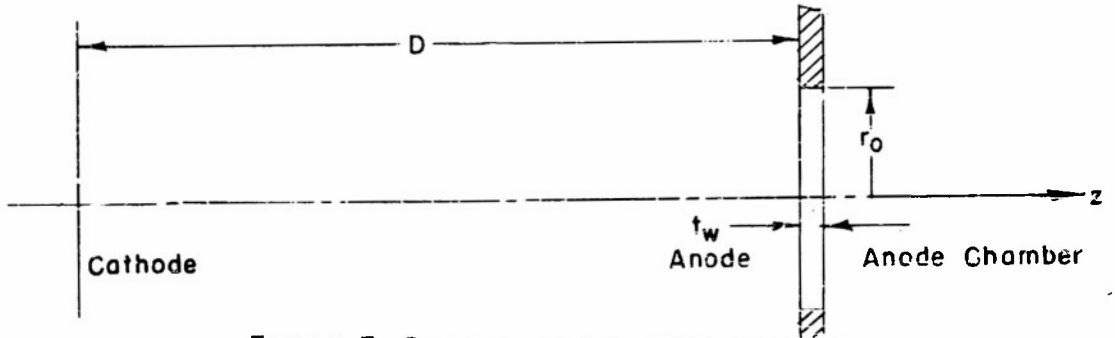

FIGURE 7 DIAGRAM OF THE ANODE ORIFICE

The average number of electrons per second that will hit the inner wall of the anode orifice (Fig. 7) is:

$$I_p = n \left(\frac{\pi k \Theta_r}{2m}\right)^{1/2} 2\pi r_o t_w$$

Taking the yield factor to be unity, secondary electrons thus produced can be expressed as:

$$I_s = \left(\frac{\pi k \Theta_r}{eV}\right)^{1/2} \frac{t_W}{\gamma_o} I_o \qquad (12)$$

In the work of secondary electron emission, it has been reasonably accepted that the angular distribution of secondary electrons follows the cosine law, independent of the angle of incidence of the primary electrons. In other words, the number of secondaries emitted per unit solid angle is greatest in the direction normal to the emitting surface and decreases with increasing angle of emergence θ as cos θ. Considering the secondary electron emission per unit area of a plane surface at

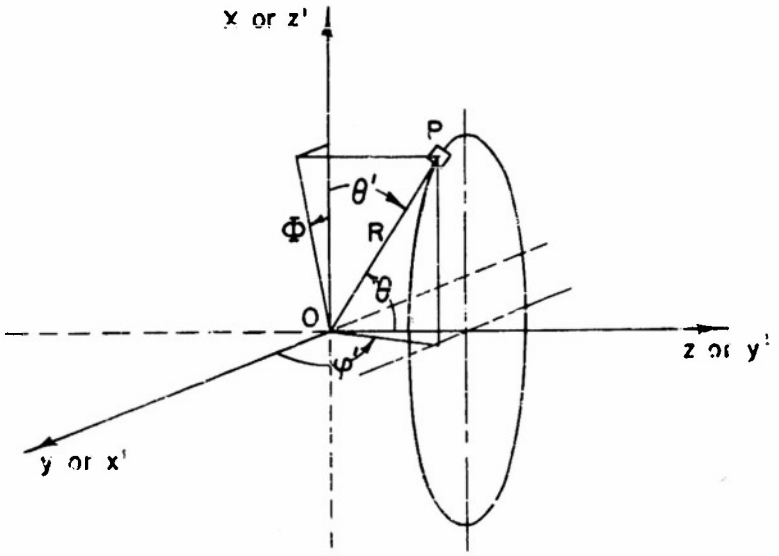

FIGURE 8 SECONDARY ELECTRON EMISSION FROM AN ORIFICE

the origin (Fig. 8) one can write

$$\frac{di_s}{d\Omega'} = h' \cos \theta'$$

in the primed coordinates, or

$$\frac{di_s}{d\Omega} = h \cos \theta \qquad (13)$$

in the unprimed coordinates, where i_s is the secondary electron current per unit area of emitting surface, Ω is the solid angle which P subtends at the origin, and h is a proportional constant.

To describe the secondary electron emission from the inner wall of an orifice, we consider that the current at P is the sum of the contributions by a small plane surface in one revolution with respect to the axis of the orifice. This is equivalent to the case where the emitting surface stays stationary but P is revolving around the Z-axis. Then the current at P would be the same as the current to the ring (generated by P in this manner) from the small plane surface at the origin. Thus, Eq. (13) is written:

$$\frac{d^2 I_s}{R^2 d\theta d\Phi} = h \sin^2 \theta \cos \Phi$$

then

$$\frac{dI_s}{R^2 d\theta} = h \sin^2 \theta \int_{-\pi/2}^{\pi/2} \cos \Phi \, d\Phi$$

or

$$\frac{dI_s}{R^2 d\theta} = 2h \sin^2 \theta$$

This describes the angle dependence of the secondary electron emission per unit area of a cylindrical surface at the origin.

Now, the secondary electron emission of an orifice can be expressed as

$$\frac{dI_s}{d\Omega} = H \sin^2 \theta \qquad (14)$$

where I_s is the secondary electron emission of an orifice, and H is a proportional constant. By normalizing the expression, one finds that

$$H = \frac{3 I_s}{8\pi R^2}$$

In deriving Eq. (14), it is assumed that $t_w << r_o << R$. Let J_s be the current density at the back wall of the anode chamber due to the secondary electrons alone, then

$$J_s(\theta) = \frac{dI_s(\theta)}{2\pi r\, dr}$$

From Eq. (14), we have

$$\frac{dI_s}{d\theta} = \tfrac{3}{4} I_s \sin^3 \theta$$

since

$$\frac{d\theta}{dr} = \frac{\cos^2 \theta}{Z}$$

then

$$J_s(\theta) = \frac{3 I_s}{8\pi Z^2} \sin^2\theta \cos^3\theta \qquad (15)$$

This gives the current density at the back wall of the anode chamber as a function of the polar angle at the center of the anode orifice, if only secondary electron emission processes are considered. In Fig. 9, the value of $\sin^2 \theta \cos^3 \theta$ is plotted against θ.

In order to see the effect of the secondary electrons in our measurements of current density distribution at the Z-plane, Eq. (15) can be written as

$$J_s(\theta) = \frac{I_o}{\pi Z^2} \left\{ \frac{3t}{8r_o} \left(\frac{\pi}{\eta}\right)^{1/2} \sin^2\theta\cos^3\theta \right\}$$

or

$$\frac{J_s(\theta)}{J(0)} = \frac{3t}{8r_o\eta} \left(\frac{\pi}{\eta}\right)^{1/2} \sin^2\theta\cos^3\theta$$

in the light of Eq. (12). In this experiment, for example,

$$\frac{t_w}{r_o} = \frac{1}{3}$$

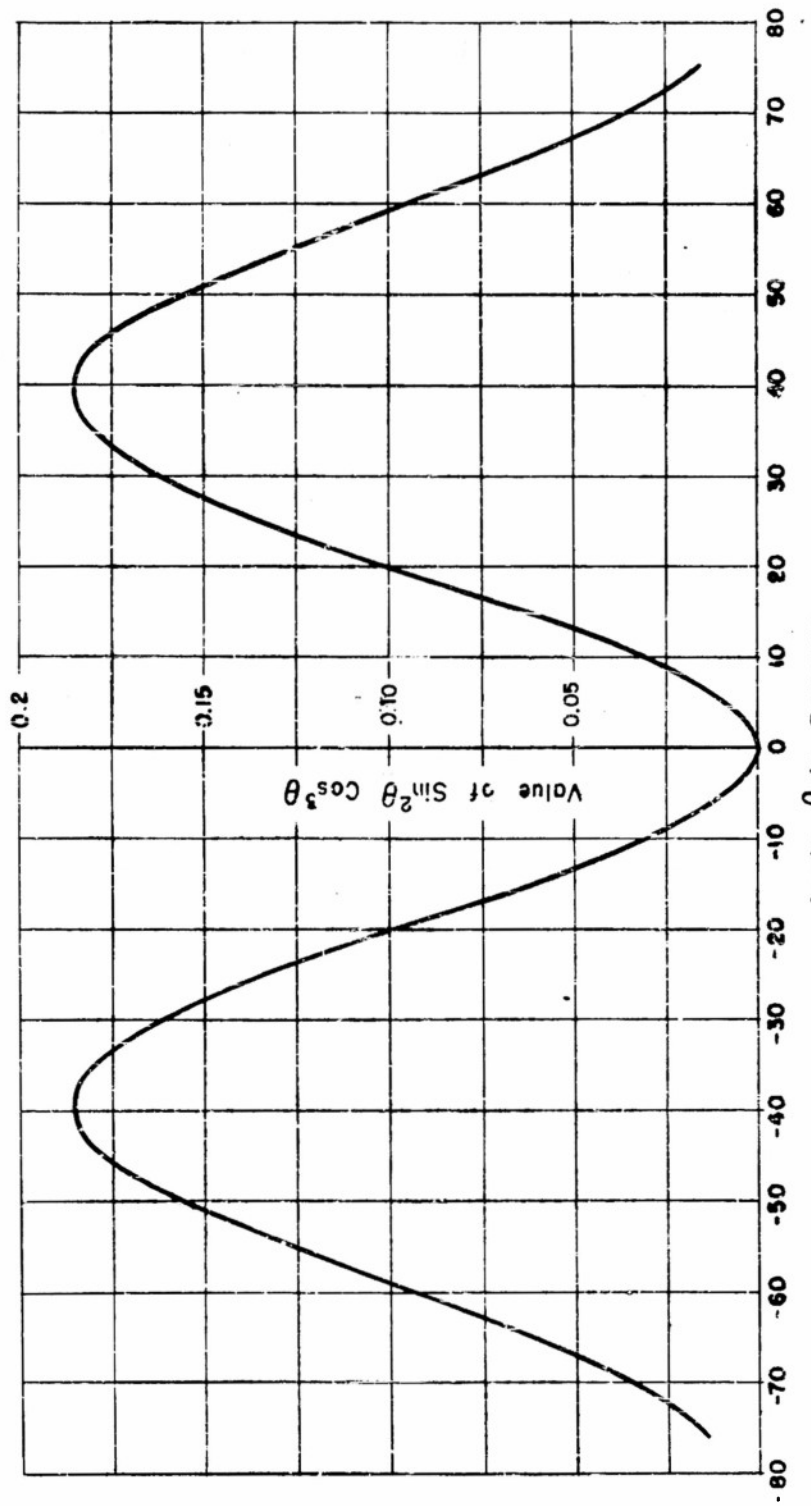

FIGURE 9 VALUE OF $\sin^2 \theta \cos^3 \theta$ AS A FUNCTION OF θ

and

$$\eta = 26.6$$

then

$$\frac{J_s(\theta)}{J(0)} \leq 3 \times 10^{-4}$$

This ratio is very small as compared with that in Eq. (4). It will be seen that the ratio, $J(\theta)/J(0)$, encountered in the measurements, is always greater than 10^{-1}. Hence, the secondary electron effect is entirely negligible in this experiment.

4.4 Conclusion

In the study of this arrangement, estimations of the aberrations have been made for each of these effects. It is rather fortunate that the beam expansion predicted from the existing electron temperature alone is much larger than all the effects arising from the aberrations. This will also be seen in the next section where the experimental results are presented. Since the current-density distribution at the back wall of the anode chamber is predominantly due to the electron temperature, the velocity spread of the emerging electrons can readily be expressed in terms of an electron temperature.

4.5 Experimental Results

Before we present the current-density measurements at the back wall of the anode chamber, it would be proper to assure that the assumptions made in the theoretical considerations are fulfilled. Particular attention has been paid to the activation of the large surface cathode, and the proper performance of the diode has been carefully checked. Measurements of the space charge flow for different cathode-anode spacings have been carried out. The results are shown in Figs. 10 and 11. The straight lines in both figures represent the theoretical Child-Langmuir space-charge law in logarithmic coordinates; first, in the form

$$i_A V^{-3/2} = \text{const} \, D^{-2}$$

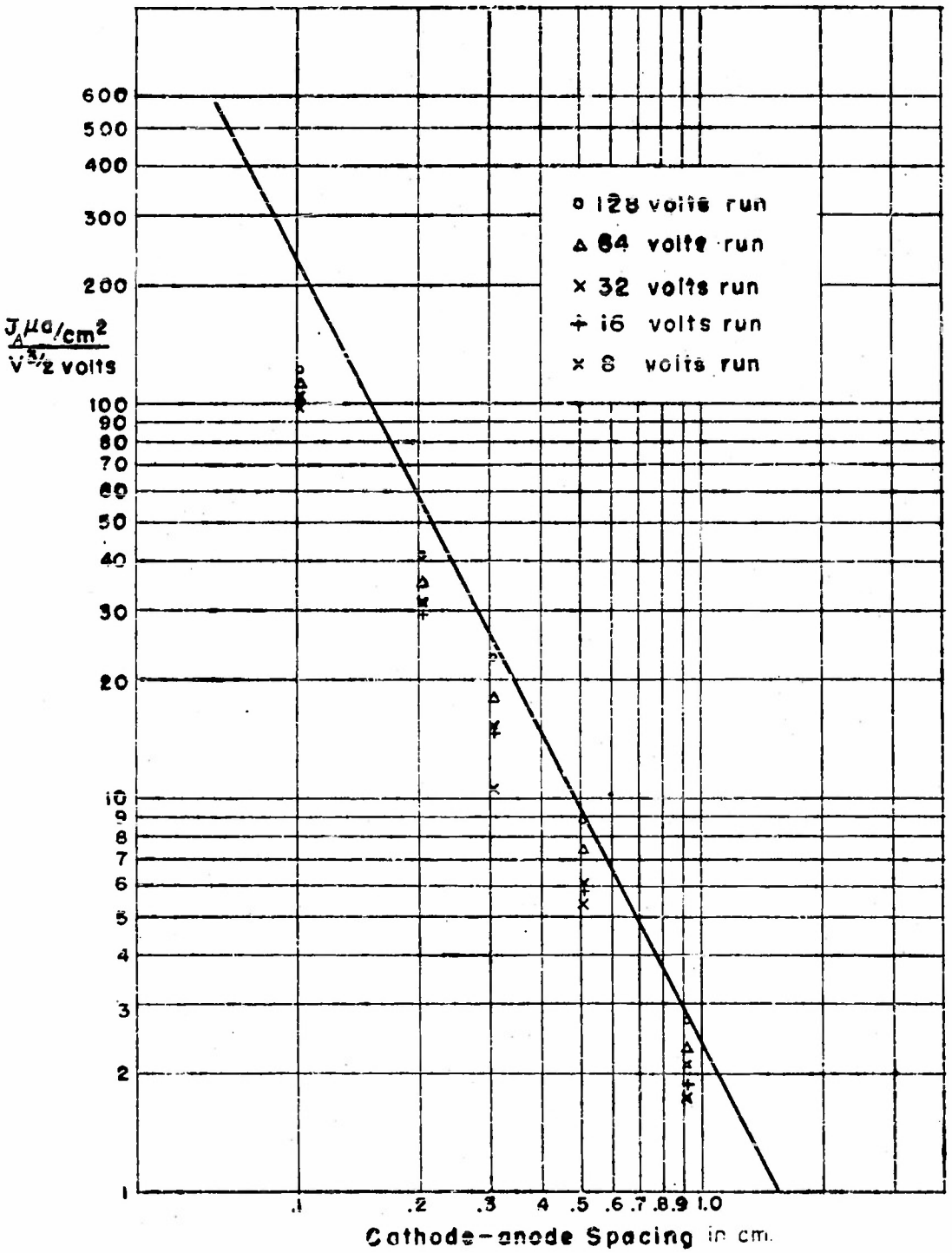

FIGURE 10 REDUCED CURRENT DENSITY AS A FUNCTION OF CATHODE-ANODE SPACING

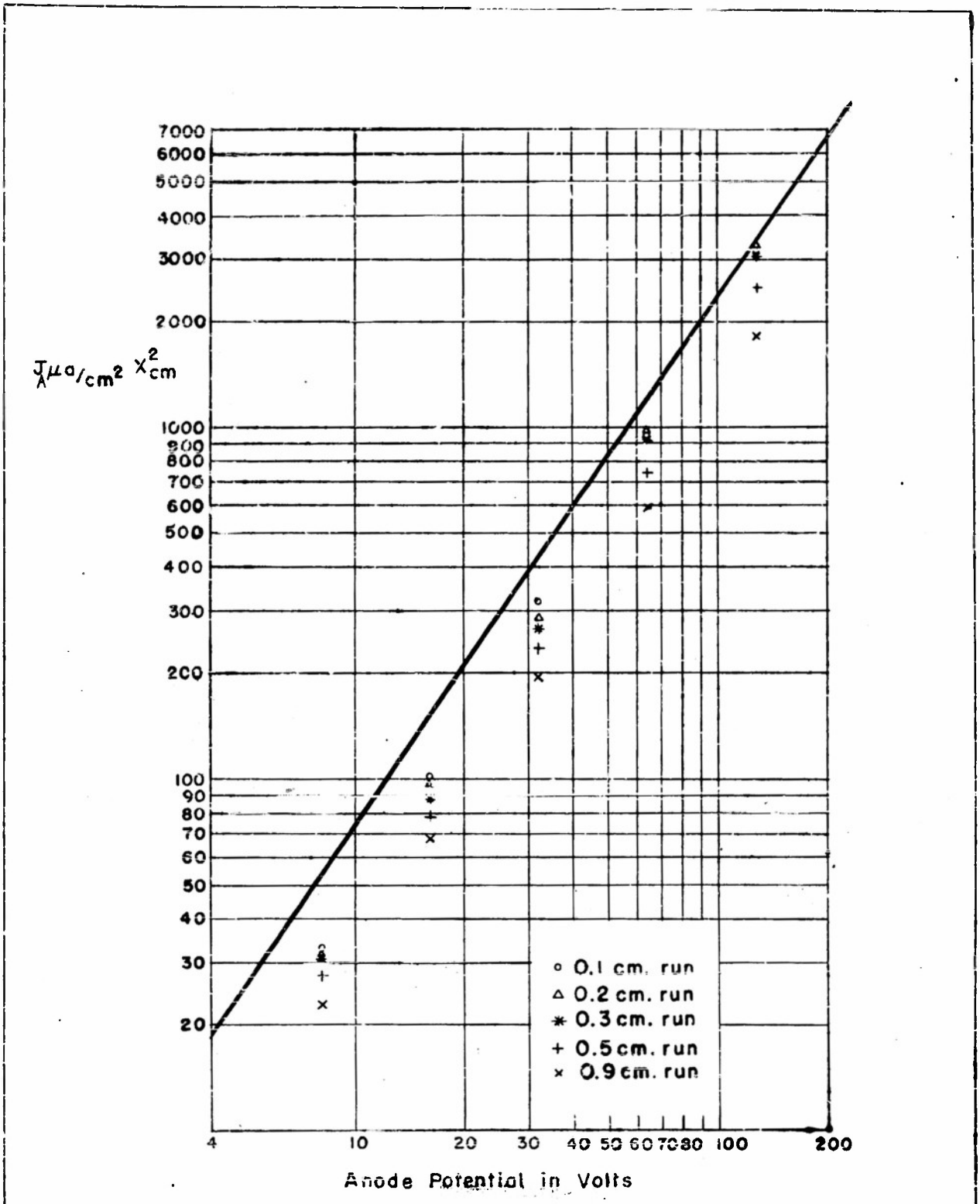

FIGURE 11 REDUCED CURRENT DENSITY AS A FUNCTION OF ANODE POTENTIAL

second, in the form

$$j_A D^2 = QV^{3/2}$$

where

j_A is the current density in $\mu a/cm^2$

V is the anode potential in volts,

D is the cathode-anode spacing in cm,

and Q is a constant, 2.335.

The points in both figures represent the observed values reduced to the corresponding units. It may be noted that the micrometer drive has a zero reading of about 0.018 cm. This would cause the last two sets of points in Fig. 10 to deviate from a straight line, but the observed values indicate very strongly that the Child-Langmuir space-charge law is definitely applicable. Since in Sections 4.1 and 4.2, the Child-Langmuir law has been used in the deductions, it is important to verify that the diode operates properly under appropriate conditions.

Having established the proper functioning of the diode with respect to its main characteristics, one may now proceed to the determination of the desired electron temperature. As was shown in Section 2 of this Part (Eqs. (4) and (6)), the electron temperature at a given point of interest is evaluated from the investigation of the current distribution on the back wall of the anode chamber. The corresponding equations were

$$\log_e \left[\frac{J(\theta)}{J(0)}\right] = -\eta\theta^2 \tag{4}$$

$$k\Theta_r = \frac{eV}{\eta} \tag{6}$$

where $J(\theta)/J(0)$ is the relative current density on the back wall of the anode chamber, θ is the polar angle, η is the slope of Eq. (4), V is the anode potential and Θ_r is the r-component electron temperature.

In order to obtain the desired data, the cathode is set at a definite temperature; with the cathode micrometer drive, the cathode is

set at a desired spacing; and a stable anode current is adjusted by arranging for an appropriate anode potential. The current distribution along the back wall of the anode chamber is then determined by measuring the current passing to the collector for different positions of the fine aperture on the running slide. With the given geometry of the anode chamber it is easy to express the position of the aperture on the running slide in polar angles θ with respect to the anode orifice. To facilitate a comparison between the experimental data and the theoretical expressions, Eqs. (4) and (6), the measured values must be expressed in terms of the logarithm of the relative current density, $J(\theta)/J(0)$, and the square of the polar angle, θ^2.

A large set of measurements have been carried out and some of the typical results are shown in Fig. 12. The points in Fig. 12 represent the measured values and show a good indication of constituting a straight line as required by Eq. (4). These results seem to indicate very strongly that the spread of the electron beam behind the anode orifice is caused by the radial velocity distribution of the electrons at the moment of entering the anode chamber, rather than by the different aberrations as lens action of the anode orifice, space charge effect, and secondary emission. For, if there were no velocity spread in the flow, the beam cross-section at the back wall of the anode chamber would (a) subtend a polar angle less than $(\theta_1 + \theta_2)$ at the center of the anode orifice, and (b) be independent of the anode potential applied. But nothing of that sort could be observed. First, the beam cross-section at the back wall of the anode chamber subtends by a far greater polar angle than $(\theta_1 + \theta_2)$ at the center of the anode orifice. Second, the beam expansion has a strong dependence on the anode potential. This makes the velocity spread of the electrons the most important factor in accounting for the beam expansion, and confirms the estimated small values of those aberrations as given in Section 4.

It was mentioned in Section 3 that in spite of different spacings between cathode and anode, the same regions of the electron flow may be considered as having the same characteristics, provided the cathode temperature and the current density in the diode are the same. Therefore, this method allows measurement of the electron temperature at any arbitrary point within a parallel plane flow which is defined by just two parameters, namely, cathode temperature and current density. In

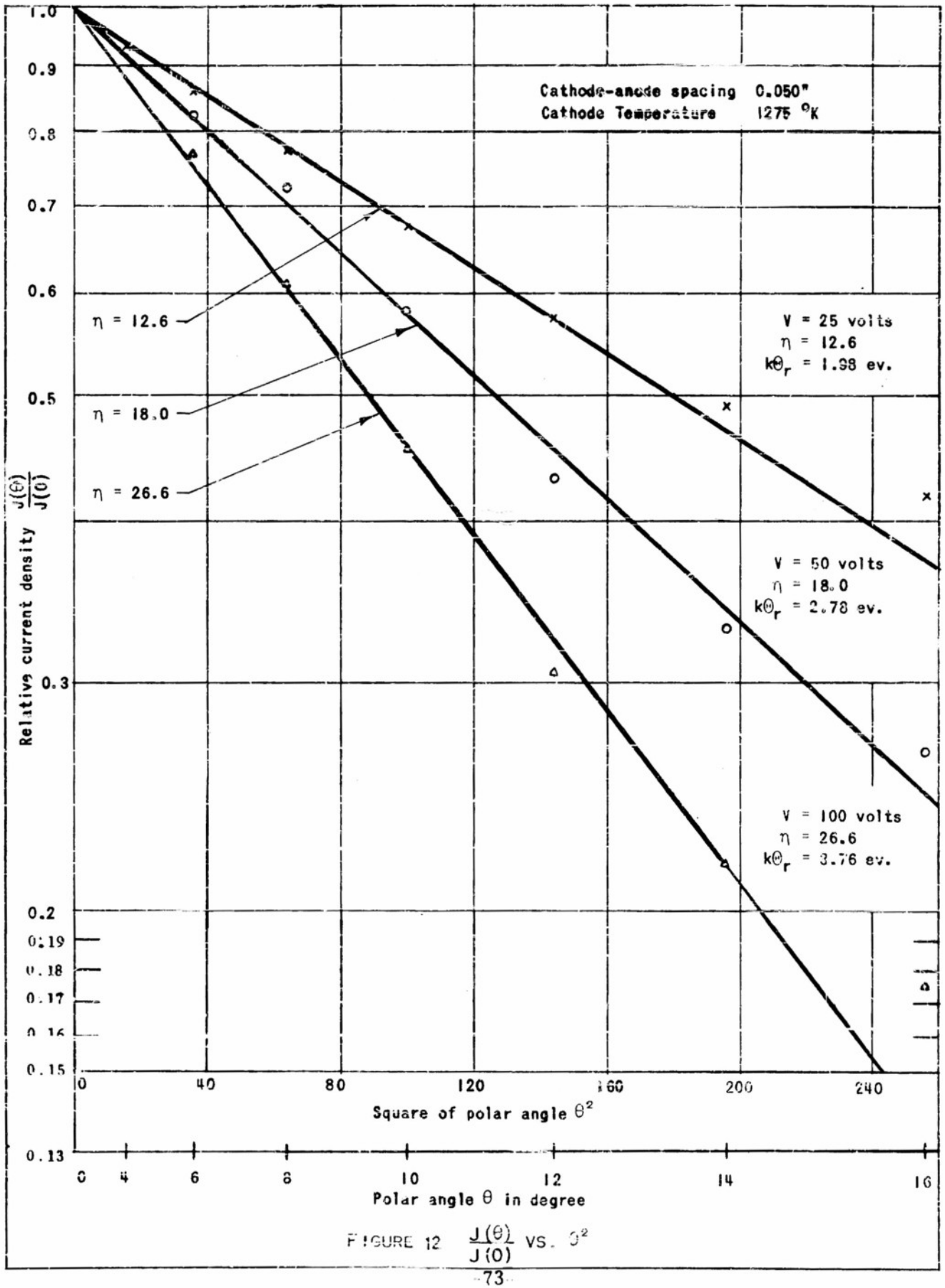

FIGURE 12 $\frac{J(\theta)}{J(0)}$ VS. θ^2

order to obtain the desired electron temperature at a given point of interest along the flow which is characterized by its cathode temperature and its current density, one has to place the anode plane at the point of interest and determine the electron temperature by observing the current distribution on the back wall of the anode chamber as described above. Varying the cathode-anode spacing and adjusting the anode potential such that the anode current remains constant gives a complete description of the electron temperature as a function of the distance from the cathode. It may be noted that the so determined electron temperature at each point of interest is an evaluation of a set of data, obtained by measuring the current distribution at the back wall of the anode chamber for the point in question, as described above.

A set of experiments was carried out to establish the relationship between the electron temperature and the distance from the cathode surface for a given cathode temperature and anode current. The results of these experiments for a constant cathode temperature of 1275°K, and for different current densities in the flow are represented in Fig. 13. One interesting fact may be immediately noted, namely, the decrease of the electron temperature with the increase of the distance from the cathode surface. This decrease of the temperature can easily be accounted for if one remembers that in the theoretical part of this report, a decrease of the temperature with increasing distance from the cathode surface was predicted for the isotropic flow where the three temperature components are equal to each other. The corresponding equation reads:

$$\Theta_r \propto v^{-2/3} \tag{I.44}$$

Although this equation establishes only a correlation between the electron temperature and the mean velocity of the electron stream at the point of consideration, it is easy to convert the expression, with the aid of the Child-Langmuir equation, into a temperature-distance relation. In Appendix II of Part I this relationship is derived and according to Eq. 2, Part II, one obtains for the isotropic flow the desired correlation between the electron temperature and the distance from the cathode surface,

$$\Theta_r \propto D^{-4/9}$$

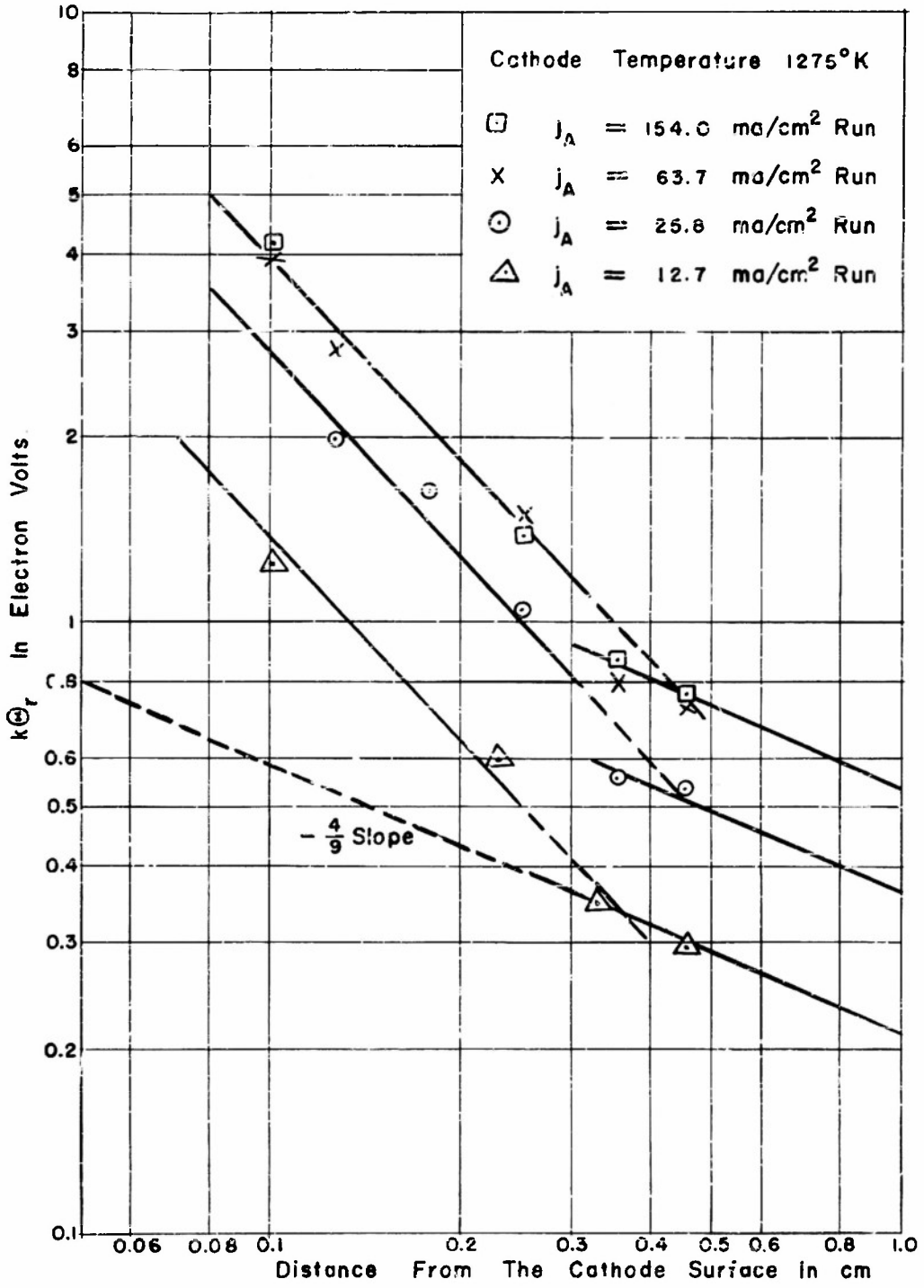

FIGURE 13 $K\Theta_r$ VS. THE DISTANCE FROM THE CATHODE SURFACE

Since the data in Fig. 13 are represented in log-log coordinates, any exponential dependency would present itself as a straight line, the slope of which would correspond to the exponent of the independent variable (see also Part 1, App. II). For comparison, a -4/9 slope representing the isotropic case is indicated in the same graph. Although for large distances there is an indication that the electron temperature may follow a -4/9 power law, for smaller distances this is obviously not the case. At this point no account can be given for the deviation from the expected dependency. Only a much more extensive experimental investigation of the region close to the cathode surface can provide sufficient data to allow further theoretical considerations. They will be presented in a later report.

It may be interesting to compare the experimental results obtained in this study with the well known fact that the electron temperature should increase with increasing plate voltage. Since in the usual experimental arrangement the cathode-anode spacing is kept constant, the above statement is equivalent to the statement that the electron temperature should increase with increasing current density. Figure 14 is obtained by arranging the experimental data such that the electron temperature is plotted against the current density with the distance as parameter. One may note that the electron temperature tends to reach an asymptotic value for high current densities.

One of the most startling findings in the experimental results of this study is the extraordinarily high electron temperature as compared to the cathode temperature. To make this point particularly clear, in Fig. 15 the electron temperature at a constant distance of 0.13 cm is plotted against the cathode temperature for two different plate voltages, 50 and 100 volts. Although the cathode temperature does not exceed 1300°K, the temperature of the electron gas at the anode orifice assumes values of the order of 10,000 to 40,000°K. Before giving an explanation of this phenomenon we should note that an agreement of the temperature of the electron gas with the temperature of the cathode is usually found by the retarding field method at low cathode temperatures. In the evaluation of the data obtained from the retarding field measurements, an important assumption is made, namely, that the space charge in the diode is negligible. Due to this assumption, the range of these measurements is usually limited to low cathode temperatures. In fact, at

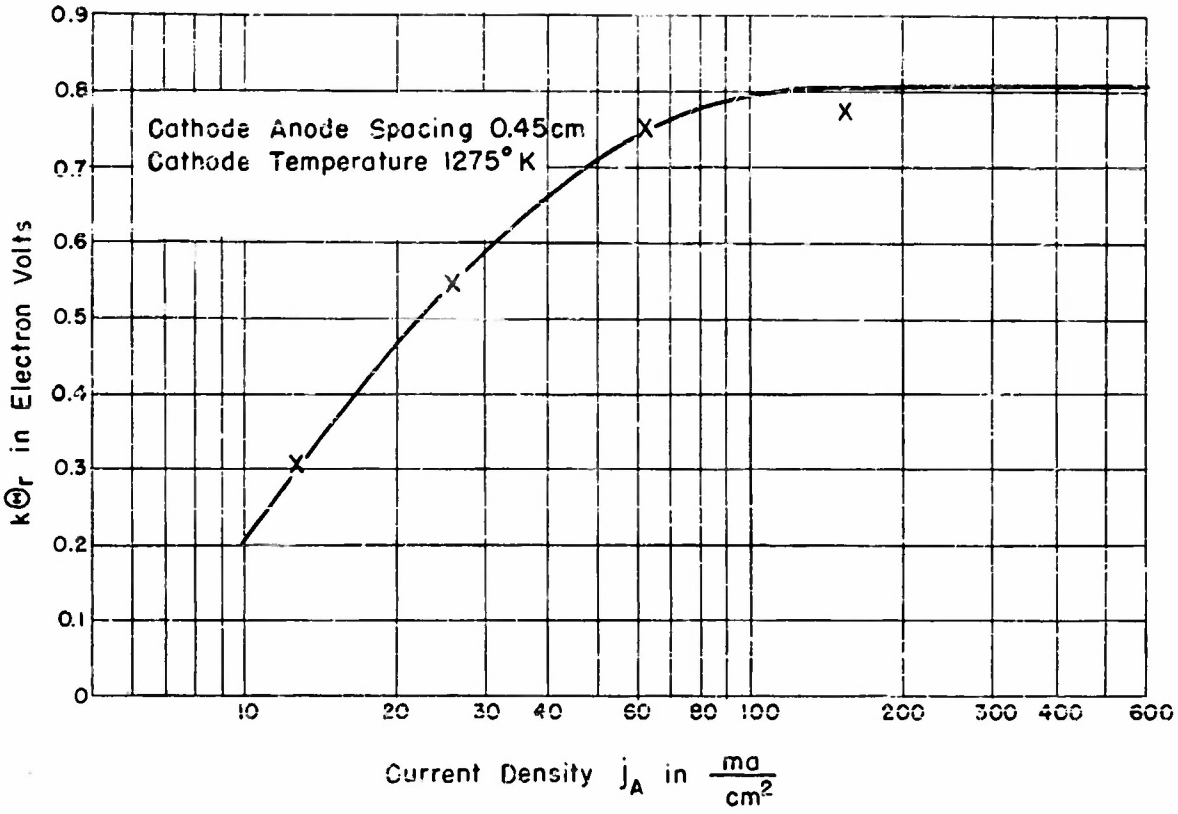

FIGURE 14 $k\Theta_r$ VS. CURRENT DENSITY

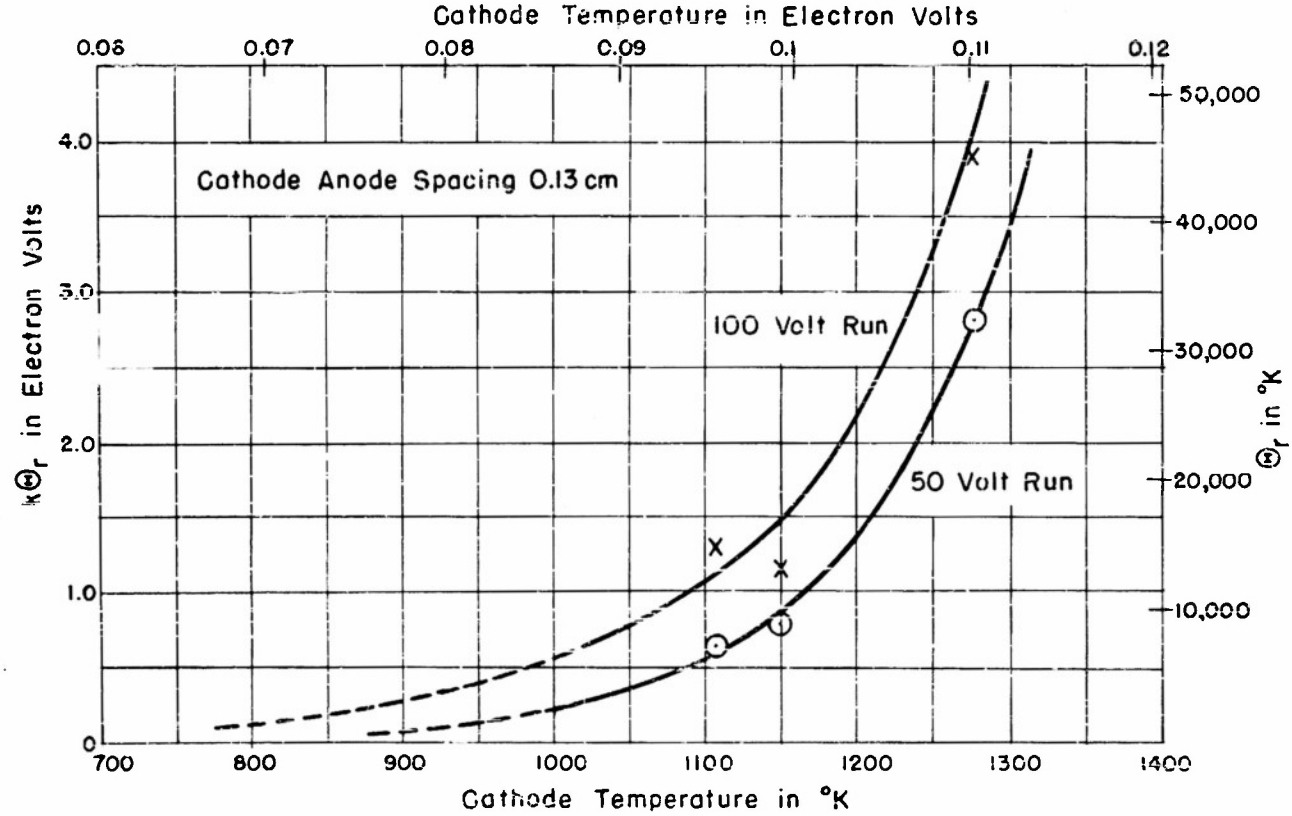

FIGURE 15 RELATION BETWEEN ELECTRON TEMPERATURE AND CATHODE TEMPERATURE

high cathode temperatures the experimental curves do not show the expected abrupt bend, hence the evaluation of the electron temperature from these curves seems rather doubtful. Since the electron temperature from high temperature cathode has not been experimentally determined, the above results do not contradict the agreement found at the low cathode temperatures.

Before concluding the experimental part, an attempt will be made to explain the extremely high temperature of the electron gas close to the cathode. This explanation will rest essentially on the experimental evidence that the temperature of the electron gas decreases sharply if the temperature of the cathode is lowered, as indicated in Fig. 15. Although the present apparatus is not sensitive enough to measure the electron temperature for very low cathode temperatures, it seems reasonable to believe that the temperature of the electron gas will approximate the cathode temperature in the lower regions. This assumption may be well supported by a closer examination of the emission mechanism of oxide-coated cathodes.

It is known that the oxide coating prepared in the conventional processes has a porous structure, the porosity ranging from 65% to about 85%[12]. Experimental evidence,[16] that the outer layers of the oxide coating are chiefly responsible for the electron emission, was found. Figure 16 may represent a schematic diagram of such an oxide-coated surface. This structure suggests that at low temperature the surface grains may possibly be responsible for the entire emission. The replacement of the electrons lost by the surface grains through the process of emission will be supplied by electrons coming from the deeper layers through a process of conduction in the oxide coating. Since the electron emission in this case may be considered as originating from the grains at the surface, the velocity spread, or the temperature of the emitted electrons, would correspond to the thermal temperature of the oxide coating as in the case of electron emission from pure metals.

Experiments[17] have shown that conduction through the oxide coating is due to two mechanisms acting in parallel--the electronic conduction through the grains, predominating at low temperatures, and the conduction through the electron gas in the pores between the grains, which is preponderant at high temperatures. Since at higher temperatures the conductivity of the coating will decrease, on the other hand the emission will rapidly increase with increased temperature, it is clear that

at elevated temperatures the conduction will lag behind the emission. With this picture in mind it is not difficult to see that at high temperatures a part of the emission may come from the electron gas in the pores between the grains. In the process of emerging from the narrow channels between the grains, the electrons will probably suffer a series of collisions with the heavy grain particles and may assume temperatures which by far exceed the temperature of the grain particles.[18]

It is interesting to note that the above explanation can also account for the fact that the electron temperature will increase if a higher anode potential is applied. In a recent paper[19] by Loosjes, Vink and Jansen, it was found that under pulsed operation the velocity spread of the emitted electrons from oxide coating would often amount to hundreds of electron volts.

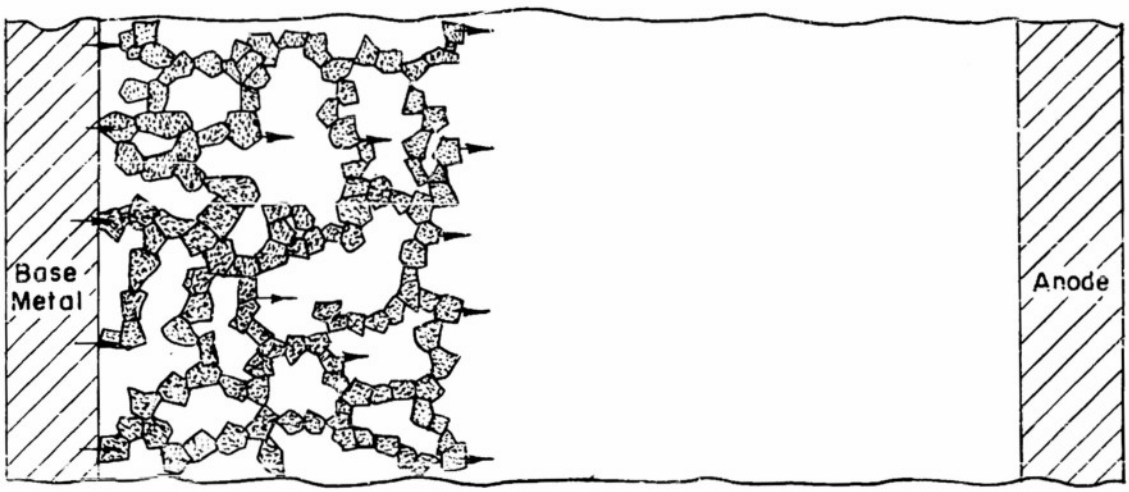

FIGURE 16 ILLUSTRATIVE DIAGRAM OF THE OXIDE COATING

BIBLIOGRAPHY

1. I. Langmuir and K. T. Compton, *Rev. Mod. Phys.*, 13, 191, (1931)
   L. Page and N. E. Adams, *Phys. Rev.*, 76, 381 (1949)
2. P. S. Epstein, *Ber. und Deut. Phys. Ges.*, 21, 85 (1919)
3. T. C. Fry, *Phys. Rev.*, 17, 441 (1921)
4. I. Langmuir, *Phys. Rev.*, 21, 219 (1923)
5. H. Goldstein, *Classical Mechanics* p. 10, Addison-Wesley Press, Inc.
6. S. Chapman and T. G. Cowling, *The Mathematical Theory of Non-uniform Gases*, Cambridge University Press (1952)
7. Taro Kihara, *Rev. Mod. Phys.*, 24, 45 (1952)
8. S. Chandrasekhar, *Principles of Stellar Dynamics, p. 7*, Chicago University Press
9. S. Chandrasekhar, *The Astrophysical Journal*, 93, 285 (1941); 94, 511 (1941)
10. C. Herring and M. H. Nichols, *Rev. Mod. Phys.*, 22, 398 (1951)
11. W. D. Nottingham, *Phys. Rev.*, 49, 78 (1936)
12. G. Herrmann and S. Wagener, *The Oxide-coated Cathode*, Chapman and Hall Ltd.
13. E. L. Ince, *Ordinary Differential Equations* , Dover Publications, Inc. (1926)
14. V. K. Zworkykin, G. A. Morton, E. G. Ramberg, J. Hillier and A. W. Vance, *Electron Optics and the Electron Microscope*, p. 444, John Wiley and Sons, Inc.
15. K. R. Spangenberg, *Vacuum Tubes*, p. 442, McGraw-Hill Book Co., Inc.
16. N. B. Hannay, D. MacNair and H. White, *J. App. Phys.*, 20, 669 (1949)
17. R. Loosjes and H. J. Vink, *Philips Techn. Rev.*, 11, 271 (1949/1950).
18. H. S. W. Massey and E. H. S. Burhop, *Electronic and Ionic Impact Phenomena*, p. 19, Oxford Clarendon Press (1952)
19. R. Loosjes, H. J. Vink and C. G. J. Jansen, *Philips Techn. Rev.* 12, 337 (1952).

Distribution List for Technical Reports
N6-ori-71 Task XIX
NR 073 162

Copies

3 Office of Naval Research
Navy Department
Washington 25, D.C.
Attn: Code 427

6 Director
Naval Research Laboratory
Washington 25, D. C.
Attn: Code 2000

1 Commanding Officer
Office of Naval Research Branch Office
1000 Geary Street
San Francisco 9, California

1 Commanding Officer
Office of Naval Research Branch Office
1030 E. Green Street
Pasadena 1, California

1 Commanding Officer
Office of Naval Research Branch Office
346 Broadway
New York, 13, New York

2 Chief, Bureau of Ships
Navy Department
Washington 25, D. C.
Attn: Code 810

1 Chief, Bureau of Aeronautics
Navy Department
Washington 25, D. C.
Attn: EL-4

1 Chief, Bureau of Ordnance
Navy Department
Washington 25, D. C.
Attn: Re4

1 Chief of Naval Operations
Navy Department
Washington 25, D. C.
Attn: Op-20X

Copies

1 Director
Naval Research Laboratory
Washington 25, D. C.
Attn: Code 2027

1 Director
Naval Research Laboratory
Washington 25, D. C.
Attn: Code 3470

1 Officer-in-Charge
Office of Naval Research
Navy #100
Fleet Post Office
New York, New York

2 Commanding Officer
Office of Naval Research Branch Office
Tenth Floor
The John Crerar Library Building
86 East Randolph Street
Chicago 1, Illinois

1 Director
Naval Ordnance Laboratory
White Oak, Maryland

1 Chief, Bureau of Ships
Navy Department
Washington 25, D. C.
Attn: Code 816

1 Chief, Bureau of Aeronautics
Navy Department
Washington 25, D. C.
Attn: EL-41

1 Chief, Bureau of Ordnance
Navy Department
Washington 25, D. C.
Attn: Re9

1 Chief of Naval Operations
Navy Department
Washington 25, D. C.
Attn: Op-371C

Copies

1 U. S. Naval Proving Ground
Dahlgren, Virginia
Attn: W. H. Benson

1 U. S. Naval Post Graduate School
Monterey, California
Attn: Prof. C.E. Menneken

3 Commanding Officer
Signal Corps Engineering Laboratories
Evans Signal Laboratory
Belmar, New Jersey
Attn: Chief, Thermionics Branch

1 Panel on Electron Tubes
Eighth Floor
346 Broadway
New York 13, New York

1 Massachusetts Institute of Technology
Laboratory for Insulation Research
Cambridge 39, Massachusetts
Attn: Prof. A. von Hippel

1 Harvard University
Cruft Laboratory
Cambridge, Massachusetts

1 Yale University
Sloane Physics Laboratory
New Haven, Connecticut
Attn: Prof. R. Beringer

2 Commanding General
Air Force Cambridge Research Center
230 Albany Street
Cambridge 39, Massachusetts
Attn: Dr. L.M. Hollingsworth

1 University of California
Electrical Engineering Department
Berkeley 4, California
Attn: Prof. J. Whinnery

1 Airborne Instruments Laboratory
160 Old Country Road
Mineola, L.I., New York
Attn: Mr. John Dyer

Copies

1 Director
Naval Electronics Laboratory
San Diego 52, California

1 U. S. Coast Guard
1300 E Street, N.W.
Washington 25, D.C.
Attn: EEE

1 Secretary, Committee on Electronics
Office of the Assistant Secretary
of Defense (Research & Development)
Department of Defense
Washington 25, D.C.

1 Massachusetts Institute of Technology
Research Laboratory of Electronics
Cambridge 39, Massachusetts
Attn: Prof. J.B. Wiesner

1 Federal Telecommunication Laboratories
500 Washington Avenue
Nutley 10, New Jersey
Attn: Head, Security Control Section

1 Yale University
Dunham Laboratory
New Haven, Connecticut
Attn: Prof. H.J. Reich

2 Commanding General
Wright Air Development Center
Wright-Patterson Air Force Base, Ohio
Attn: Electronics

1 Polytechnic Institute of Brooklyn
Microwave Research Institute
55 Johnson Street
Brooklyn 1, New York
Attn: Prof. Ernst Weber

1 Raytheon Manufacturing Company
Waltham, Massachusetts
Attn: H.R. Argento

1 Sperry Gyroscope Company
Great Neck, L.I., New York
Attn: Mr. R.L. Wathen

Copies

1 Microwave Laboratory
Stanford University
Stanford, California

Attn: Dr. E.L. Ginzton

1 General Electric Company
Research Division
Schenectady, New York

Attn: Mr. E.D. McArthur

5 ASTIA Document Service Center
Knott Building
Dayton 2, Ohio

1 Commanding Officer
Signal Corps Electronics Research Unit
9560th TSU, P. O. Box 205
Mountain View, California

Copies

1 Electronics Research Laboratory
Stanford University
Stanford, California

1 Bell Telephone Laboratories
Murray Hill, New Jersey

Attn: Dr. J.R. Pierce

1 Office of Technical Services
Department of Commerce
Washington, D.C.